

**FINAL REPORT**

(Project SR-103)

on

**TENSILE TESTS OF LARGE SPECIMENS REPRESENTING THE  
INTERSECTION OF A BOTTOM LONGITUDINAL WITH A  
TRANSVERSE BULKHEAD IN WELDED TANKERS**

by

L. K. IRWIN and W. R. CAMPBELL  
National Bureau of Standards

Under Bureau of Ships Project NS-731-034

for

**SHIP STRUCTURE COMMITTEE**

Convened by  
The Secretary of the Treasury

*Member Agencies—Ship Structure Committee*

Bureau of Ships, Dept. of Navy  
Military Sea Transportation Service, Dept. of Navy  
United States Coast Guard, Treasury Dept.  
Maritime Administration, Dept. of Commerce  
American Bureau of Shipping

*Address Correspondence To:*

Secretary  
Ship Structure Committee  
U. S. Coast Guard Headquarters  
Washington 25, D. C.

SERIAL NO. **SSC-68**  
BuShips Project NS-731-034

**JANUARY 18, 1954**

# SHIP STRUCTURE COMMITTEE

## MEMBER AGENCIES:

BUREAU OF SHIPS, DEPT. OF NAVY  
MILITARY SEA TRANSPORTATION SERVICE, DEPT. OF NAVY  
UNITED STATES COAST GUARD, TREASURY DEPT.  
MARITIME ADMINISTRATION, DEPT. OF COMMERCE  
AMERICAN BUREAU OF SHIPPING

## ADDRESS CORRESPONDENCE TO:

SECRETARY  
SHIP STRUCTURE COMMITTEE  
U. S. COAST GUARD HEADQUARTERS  
WASHINGTON 25, D. C.

January 18, 1954

Dear Sir:

As part of its research program related to the improvement of hull structures of ships, the Ship Structure Committee is sponsoring an investigation on design details at the National Bureau of Standards. Herewith is a copy of the Final Report, SSC-68, of the investigation, entitled "Tensile Tests of Large Specimens Representing the Intersection of a Bottom Longitudinal with a Transverse Bulkhead in Welded Tankers" by L. K. Irwin and W. R. Campbell.

Any questions, comments, criticism or other matters pertaining to the Report should be addressed to the Secretary, Ship Structure Committee.

This Report is being distributed to those individuals and agencies associated with and interested in the work of the Ship Structure Committee.

Yours sincerely,



K. K. COWART  
Rear Admiral, U. S. Coast Guard  
Chairman, Ship Structure Committee

FINAL REPORT  
(Project SR-103)

on

TENSILE TESTS OF LARGE SPECIMENS REPRESENTING THE INTERSECTION  
OF A BOTTOM LONGITUDINAL WITH A TRANSVERSE BULKHEAD IN  
WELDED TANKERS

by

L. K. Irwin and W. R. Campbell  
National Bureau of Standards

under

Department of the Navy  
BuShips Project No. NS-731-034

for

SHIP STRUCTURE COMMITTEE

## TABLE OF CONTENTS

	Page
List of Figures. . . . .	ii
List of Tables . . . . .	iv
Forward. . . . .	v
Abstract . . . . .	vii
Introduction . . . . .	1
Specimens. . . . .	4
Test Equipment and Instruments . . . . .	7
Testing Machine and Fixtures. . . . .	7
Resistance Strain Gage Instrumentation. . . . .	9
Temperature Control Apparatus . . . . .	11
Extensometers . . . . .	11
Test Procedures. . . . .	12
Calculations . . . . .	14
Results of Tests at Room Temperature . . . . .	15
Elastic Test of a Through Longitudinal. . . . .	15
Elastic Tests of Nine Interrupted Longitudinals . . . . .	18
Elastic Tests of Four Through-Bracket Longitudinals . . . . .	25
Results of Low Temperature Tests . . . . .	31
Test to Failure of a Through Longitudinal . . . . .	31
Tests to Failure of Fourteen Interrupted Longitudinals. . . . .	36
Tests to Failure of Four Through-Bracket Longitudinals. . . . .	44
Discussion . . . . .	53
Summary. . . . .	59
Recommendations on Future Work. . . . .	62
References . . . . .	64
Appendix . . . . .	65

## LIST OF FIGURES

<u>No.</u>	<u>Title</u>	<u>Page</u>
1.	The intersection of shell plate, bottom longitudinal and longitudinal bulkhead with a transverse bulkhead in T-2 tankers. . . . .	2
2.	Details of nineteen bottom longitudinal tensile specimens . . . . .	5
3.	Details of specimen 2A with welding notes and instructions for attaching pulling head. . . . .	8
4.	Location of strain gages and thermocouples on specimens 1A and 1 <sup>4</sup> A . . . . .	10
5.	Laboratory setup for room temperature test of specimen 11A . . . . .	13
6.	Laboratory setup for a low temperature test to failure . . . . .	13
7.	Specimen OA, principal stresses at 160 kips load. Minor principal stresses less than 1.0 kip/in <sup>2</sup> not shown . . . . .	17
8.	Specimen OA, axial stresses on the bottom plate and longitudinal adjacent to the transverse bulkhead. . . . .	19
9.	Specimens 1A, 2A and 3A, principal stresses at 160 kips load. Minor principal stresses less than 1.0 kip/in <sup>2</sup> not shown . . . . .	20
10.	Axial stress distribution on the bottom plate and longitudinal, section A-A, of specimens 1A, 2A and 3A. . . . .	22
11.	Axial stress distribution on the bottom plate and bracket, section B-B, specimens 1A, 2A and 3A . . . . .	24
12.	Specimens 1 <sup>4</sup> A and 1 <sup>5</sup> A, principal stresses at 160 kips load. Minor principal stresses less than 1.0 kips/in <sup>2</sup> not shown. . . . .	26
13.	Axial stress distribution on bottom plate and through-bracket, section B-B, specimens 1 <sup>3</sup> A, 1 <sup>4</sup> A and 1 <sup>5</sup> A. . . . .	28

<u>No.</u>		<u>Page</u>
14.	Axial stress distribution on bottom plate, section C-C, specimens 13A, 14A and 15A. . . . .	29
15.	Axial stress distribution on bottom plate and longitudinal, section D-D, specimens 13A, 14A and 15A . . . . .	30
16.	Specimen OA immediately after fracture. Maximum load 1,113 kips. . . . .	33
17.	Axial strain distribution on the bottom plate and longitudinal, section B-B, of specimen OA. . . . .	34
18.	Specimen 10A immediately after fracture. Maximum load: 960 kips. . . . .	37
19.	Axial strain distribution on the bottom plate and longitudinal, section A-A, of specimens 1A, 2A and 3A . . . . .	39
20.	Axial strain distributions on the bottom plate and bracket, section B-B, of specimens 1A, 10A, 2A, 2A4 and 3A . . . . .	41
21.	Energy to fracture versus test temperature for eight interrupted specimens of 1A design. (Straight line fitted by the method of least squares) . . . . .	45
22.	Upper-- Specimen 14A immediately after fracture. Maximum load: 1,144 kips. Lower-- Specimen 15A immediately after fracture. Maximum load: 799 kips. . . . .	47
23.	Axial strain distributions on the bottom plate and bracket, section B-B, of specimens 13A, 14A and 15A. . . . .	48
24.	Axial strain distributions on the bottom plate, section C-C, of specimens 13A, 14A and 15A . . . . .	50
25.	Axial strain distributions on the bottom plate and longitudinal, section D-D, of specimens 13A, 14A and 15A. . . . .	52
26.	Load versus over-all axial extension relations for specimens OA, 1A5, 2A and 14A. Data represented here were not adjusted for differences in cross-sectional area of specimens. . . . .	58

List of Tables

<u>No.</u>		<u>Page</u>
1.	Descriptions of Nineteen Bottom Longitudinal Specimens. . . . .	6
2.	Measurements and Results of Elastic Tests. Machine Load: 160,000 lb. . . . .	16
3.	Results of Low Temperature Tests . . . . .	35
4.	Chemical Composition of Plates in Nineteen Longitudinal Specimens. . . . .	66
5.	Mechanical Properties of Steel Plates in Nineteen Longitudinal Specimens . . . . .	68

## FOREWORD

Ship Structure Committee Project SR-103, Static Tests of Design Details, was initiated at the National Bureau of Standards for the purpose of studying two particular structural connections peculiar to welded tankers of the T-2 type. These two connections were (a) the intersection of a longitudinal bulkhead with a transverse bulkhead and (b) the intersection of a bottom (interrupted) longitudinal with a transverse bulkhead. The over-all project, which began in 1947, was divided into three phases as the investigation progressed.

The first phase of the program was concerned with tensile tests of sub-scale interrupted longitudinals of the original T-2 tanker design, together with longitudinals involving service modifications of the T-2 design. The results of this work were published in The Welding Journal<sup>(1)</sup>.

The second phase of the project was concerned with tensile tests of full-scale bulkhead intersection specimens of the original T-2 design, together with service variations of the original design. The results of this phase of the program were also published in The Welding Journal<sup>(2)</sup>.

This final report is concerned with tensile tests of

full-scale interrupted longitudinals to expand and verify the results obtained from the sub-scale specimens. Also certain experimental and new designs of the bottom longitudinal-transverse bulkhead connection were included in the third phase of the project.

## ABSTRACT

Investigations of three discrete designs of a bottom longitudinal connection at a bulkhead were made to furnish information on their relative mechanical behavior when loaded in tension. One through longitudinal, fourteen interrupted longitudinals, and four through-bracket longitudinals were tested. The through longitudinal was of experimental design; the interrupted longitudinals were of the basic T-2 tanker design and two major modifications of this design; and the through-bracket longitudinals were of a Navy oiler design and one specimen of a commercial tanker design. The nineteen specimens were fabricated of ship plate using shipyard procedures.

Room temperature tests were made to study elastic stress distributions and stress concentrations on critical sections of one or more specimens of each design. The specimens were tested to failure near 0°F or other selected temperatures below room temperature to determine maximum load, over-all elongation, and energy to fracture. Tests to failure at temperatures above and below 0°F were made to determine the effect of temperature on mode of fracture and energy absorption.

The maximum stress ratios (concentrations) measured on the section adjacent to the transverse bulkhead were 1.2 on

the through longitudinal, 2.1 to 2.8 on the interrupted longitudinals, and 1.6 to 1.9 on the through-bracket longitudinals, except for one specimen on which the stress ratio was 2.3. These stress concentrations were a rough measure of the inability of the longitudinals to absorb energy when tested to failure.

All specimens failed with cleavage fractures after varying amounts of plastic deformation. Generally the energy to fracture increased with test temperature. Results of the tests to failure near 0°F indicate that the modifications to the basic T-2 design were beneficial, increasing the capacity of the interrupted longitudinals to absorb the energy of deformation. Comparisons of maximum load, over-all elongation, and energy to fracture for the three longitudinal designs indicate that qualitatively the order of merit for this connection is (1) through longitudinal of experimental design, (2) through-bracket longitudinal of Navy oiler design and (3) modified interrupted longitudinals for T-2 tankers. Additional tests are needed to determine whether the superior performance of the through longitudinal design can be maintained when the necessary modifications for tanker service are introduced.

# TENSILE TESTS OF LARGE SPECIMENS REPRESENTING THE INTERSECTION OF A BOTTOM LONGITUDINAL WITH A TRANSVERSE BULKHEAD IN WELDED TANKERS

## 1. INTRODUCTION

Welded merchant vessels built before and early in World War II suffered fractures in the hull plating and deck which were not readily explained. Numerous major casualties occurred in one type of these vessels, T-2 tankers, when the bottom hull was sustaining large tensile loads. Some of the sources of hull fractures were at structural discontinuities or "mechanical notches" caused by interrupting the longitudinal hull stiffeners at intersections with transverse bulkheads. This connection, which was repeated more than 100 times in each T-2 tanker, is illustrated schematically in Figure 1. Several modifications of the details of this connection were made in attempts to improve its performance.

A preliminary investigation of design details of four interrupted longitudinal specimens with reduced cross section and four bulkhead intersection specimens has been previously reported<sup>(1,2)</sup>.

This report is concerned with tests of nineteen welded steel specimens representing the intersection of a bottom longitudinal with a transverse bulkhead in welded tankers. Fourteen full-size specimens of the interrupted longitudinal design for T-2 tankers were tested. Also four specimens

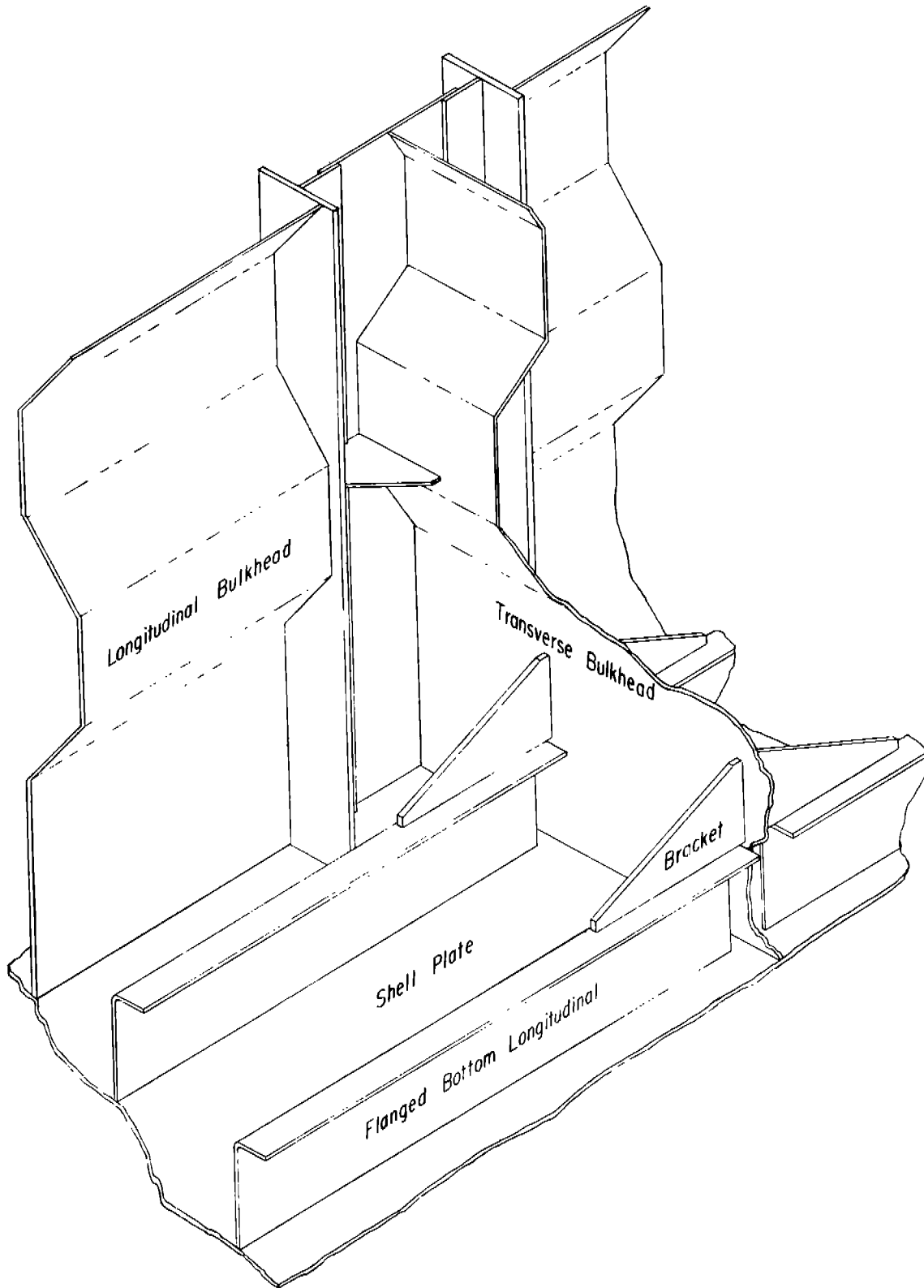


Fig. 1. The intersection of shell plate, bottom longitudinal and longitudinal bulkhead with a transverse bulkhead in T-2 tankers.

involving two recent through-bracket designs for this intersection and an experimental through longitudinal design were investigated.

The purpose of this investigation was to study the load carrying capacity, stress distribution, and energy absorption ability of the original interrupted longitudinal design, those modifications of this design in service, and a few practical modifications which were intended to increase the reliability of tankers in service. Also, it was desired to provide experimental data which might be used to improve other designs of this connection.

As tests simulating exact shipboard conditions were impractical with available test equipment, the specimens were tested in tension to simulate the action of sagging moments on the hull girder. Stress distribution studies at room temperature, strain distribution studies to failure, and over-all centerline extension measurements were made to evaluate and compare the different specimens. Tests to failure were made in most cases with the temperature of the specimen near 0°F to insure that the steel was fractured below its ductile to brittle transition temperature. Tests of some interrupted longitudinal specimens were made at other selected temperatures less than room temperature to study the effect of temperature on the mode of failure.

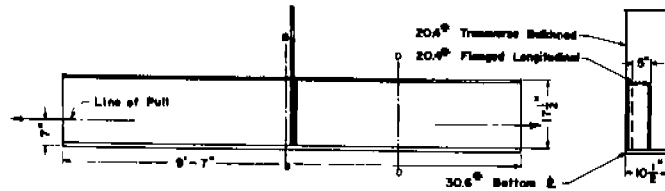
Comparisons of peak stresses and strains on critical

sections maximum load, axial extension and energy to fracture were made to establish the relative order of worth of the longitudinals. In the case of welded hatch corners on ships, the relatively good correlation of energy absorption, determined in the laboratory, with service experience<sup>(3)</sup> indicates that energy absorption can be used as a reliable criterion for classifying different designs of a complicated welded structure having inherent mechanical notches. Therefore, energy to fracture values are used in this report to indicate the relative worth of the various longitudinal designs.

## 2. SPECIMENS

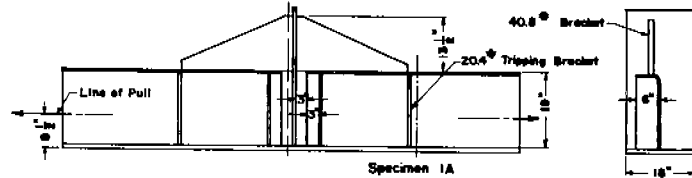
Nineteen specimens representing details of a bottom longitudinal intersecting a transverse bulkhead were tested. These specimens are shown in Figure 2 and are described in some detail in Table 1. The over-all length of the test section and pulling heads, approximately 16 ft., was determined primarily by the dimensions of the testing machine. This length of specimen was arbitrarily maintained to facilitate comparisons of over-all extension and energy to fracture.

The through longitudinal specimen OA was designed to provide a reference for evaluating the results of other specimens. The fourteen interrupted longitudinal specimens were similar to T-2 tanker construction as far as dimensions,

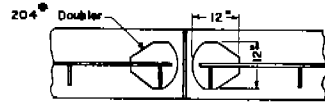
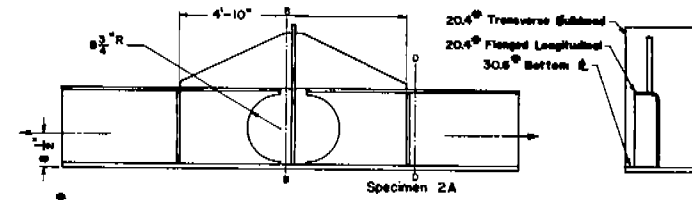


Specimen No.	No. Tested
OA	1

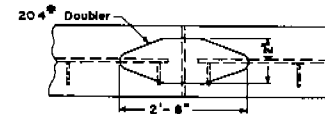
Through Longitudinal



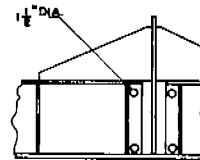
Specimen No.	No. Tested
1A	6
2A	4
3A	1
10A	1
11A	1
12A	1



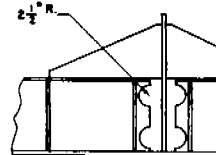
Specimen 3A-Inside View of Hull



Specimen 12A-Outside View of Hull

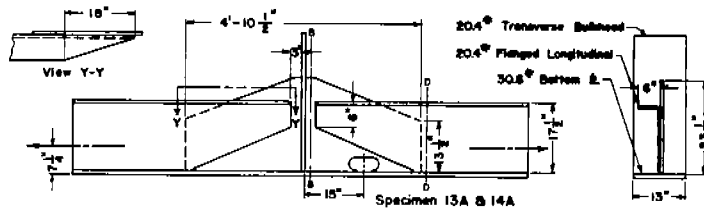


Specimen 10A

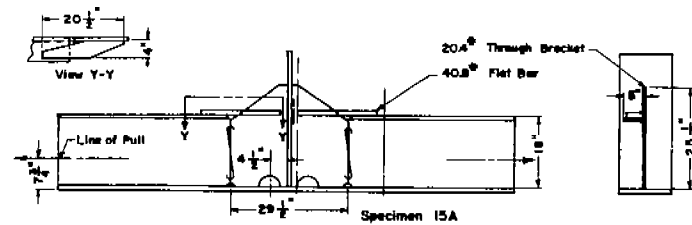


Specimen 11A

Interrupted Longitudinals



Specimen No.	No. Tested
13A	2
14A	1
15A	1



Through Bracket Longitudinals

Fig. 2. Details of nineteen bottom longitudinal tensile specimens.

Table 1 - Descriptions of Nineteen Bottom Longitudinal Specimens

Spec. No.	Type	Service	Remarks
0A	Through Long'l	Experimental	Designed to furnish a reference for comparing other designs of longitudinal connection. A continuous structure with minimum mechanical notches.
*****			
1A	Interrupted Long'l	T-2 Tanker	Original T-2 design. Relatively rigid with pronounced notches at the ends of the longitudinal web in the bottom plate and on the lower edge of the 40.8# bracket.
1A2	Interrupted Long'l	T-2 Tanker	
1A3	Interrupted Long'l	T-2 Tanker	
1A4	Interrupted Long'l	T-2 Tanker	
1A5	Interrupted Long'l	T-2 Tanker	
1A6	Interrupted Long'l	T-2 Tanker	
10A	Interrupted Long'l	Experimental	Similar to 1A specimens with small holes in ends of longitudinal web to ease notch effects.
11A	Interrupted Long'l	Experimental	Similar to 1A specimens with small cut outs in ends of longitudinal web to ease notch effects.
2A	Interrupted Long'l	Modified T-2 Tanker	T-2 design made more flexible in the intersection by removing material in web of longitudinal and eliminating the tripping brackets nearest the transverse bulkhead.
2A2	Interrupted Long'l	Modified T-2 Tanker	
2A3	Interrupted Long'l	Modified T-2 Tanker	
2A4	Interrupted Long'l	Modified T-2 Tanker	
3A	Interrupted Long'l	Modified T-2 Tanker	Stress concentrations in bottom plate reduced by using doubler under end of longitudinal.
12A	Interrupted Long'l	Experimental	Stress concentrations in bottom plates reduced by doubler on the outside to cover the area of the ends of the longitudinal.
*****			
13A	Through-Bracket Longitudinal	Navy Oiler	Represents structurally but not in exact detail the connection in one design of Navy Oiler. Structure essentially continuous with reduced stress raisers.
13A2	Through-Bracket Longitudinal	Navy Oiler	
14A	Through-Bracket Longitudinal	Navy Oiler	
15A	Through-Bracket Longitudinal	Commercial Tanker	Approximate details of the connection in one design of commercial tanker. Flat bar tying flange of longitudinal to through bracket acts as stress raiser.

plate thickness, material, and welding procedures were concerned. Three of the four through-bracket longitudinals represented a design of longitudinal in one type of Navy oiler, and the other through-bracket longitudinal was a design used in certain commercial tankers. Figure 2 shows that the term "through-bracket" refers to the relative degree of continuity. All specimens had some member continuous through the transverse bulkhead.

Material variations between specimens were minimized by procuring 30.6# steel plates of one heat and by making 40.8# components from one plate. The 40.8# bracket in specimen 1A was from the same heat as the 30.6# plates. All 20.4# material for these specimens was yard stock ship plate. The chemical compositions and mechanical properties of the steel plates are given in the Appendix.

Generally, weld sizes and procedures designated in the original design were followed in the fabrication of specimens. Fabrication under shipyard conditions was carried out by the Curtis Bay Coast Guard Yard. Details of specimen 14A as submitted to the shop for fabrication are shown in Figure 3.

### 3. TEST EQUIPMENT AND INSTRUMENTS

#### 3.1 Testing Machine and Fixtures

A horizontal Emery testing machine with a capacity in tension of 1,150 kips was used for these tests. The accuracy of this machine was of the order of 0.5 per cent of the indicated load.



Pulling heads designed to fit the interrupted longitudinal specimens were welded to the ends of the longitudinal and bottom plate. Pins and straps fastened the pulling heads to eyebars gripped in the heads of the testing machine. A schematic representation of a pulling head attached to a specimen is shown in Figure 3. During fabrication special care was used to align the pulling heads with the proper axes of the specimens.

### 3.2 Resistance Strain Gage Instrumentation

Resistance strain gages were attached on all specimens and waterproofed. Except where space was restricted, SR-4 type A-3 single element gages and AR-2 rosettes were used and will be referred to throughout this report. When it was required to locate gages in limited space, A5-1 and A-7 single element gages and AR-7 rosettes were used. Strain readings were taken using portable SR-4 strain indicators. The manufacturer's gage factors were matched for all gages attached to a particular specimen or, if this was not practical, corrections to the indicated strains of the unmatched gages were made in the computations.

One or more specimens of each design and type was gaged extensively to determine stress and strain distributions on various cross sections. Typical gage locations on fully gaged specimens are shown for specimens 1A and 14A in Figure 4.

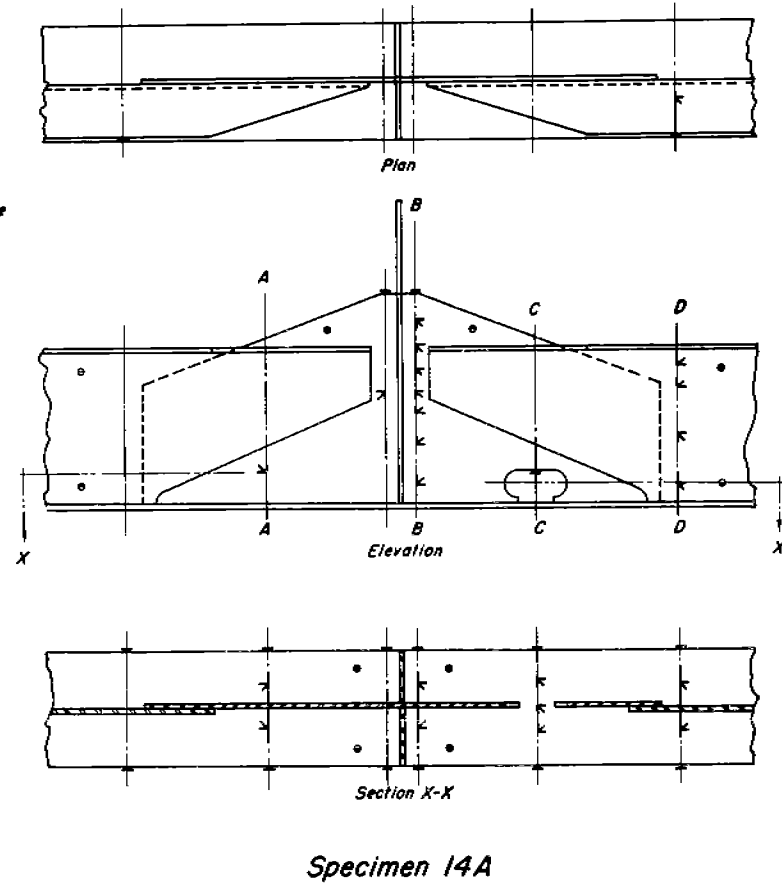
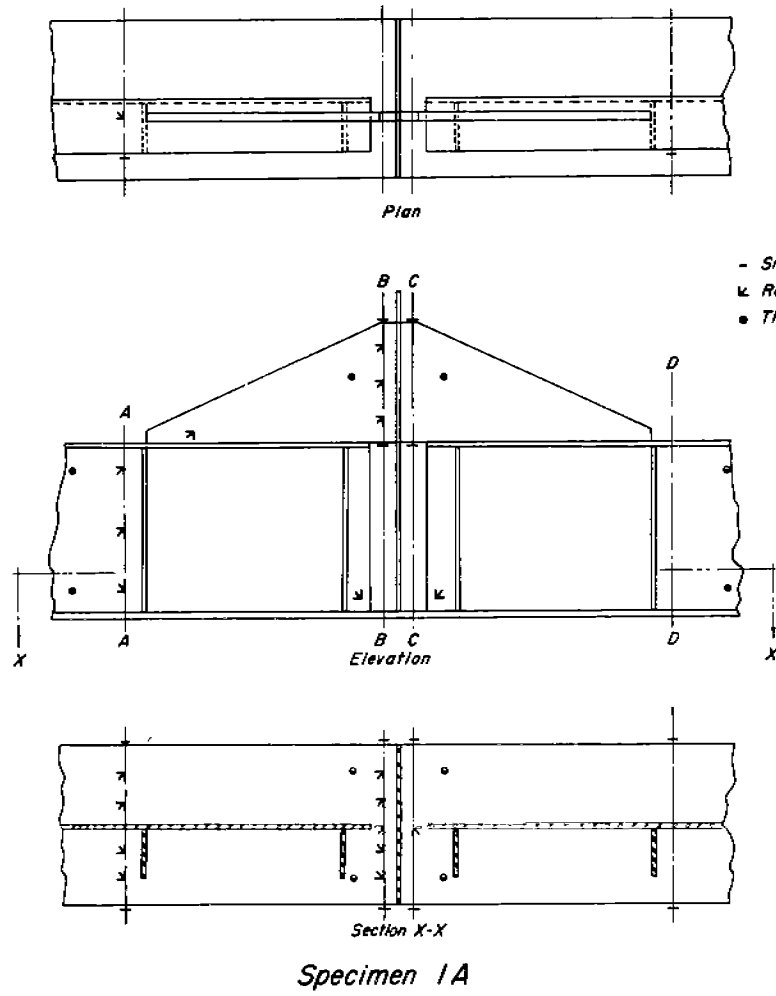


Fig. 4. Location of strain gages and thermocouples on specimens 1A and 14A.

Except for edge gages, each gage symbol represents two gages, one on each side of the specimen in similar locations. When repeated tests of a particular type of specimen were made, only points and sections of special interest were gaged. On some specimens only check gages were attached to pick up significant variations in mechanical behavior. The number of gage elements ranged from 9 to 180 per specimen.

### 3.3 Temperature Control Apparatus

An open top box of insulating board was constructed around seven specimens for tests to failure. Solid carbon dioxide distributed in the box was used as the coolant. The twelve remaining specimens were fully enclosed in boxes of insulating board to obtain better temperature control. A cooling system which recirculated gas from solid carbon dioxide was connected to these boxes. During the low temperature tests the welds connecting the specimens to the pulling heads were heated with infrared lamps or electric strip heaters.

Ten copper-constantan thermocouples were installed on each specimen as shown in Figure 4 for low temperature determinations. It is estimated that observed temperatures differed from true temperatures by less than 1°F.

### 3.4 Extensometers

Two dial extensometers having gage lengths of approximately 132 inches for determining over-all axial extension

to failure were attached to the pulling heads of each specimen through rigid posts. The dials were read to 0.001 in. increments of extension. The use of two dials made it possible to correct the results of extension measurements for specimen rotation about a horizontal axis perpendicular to the line of pull as discussed in the authors' closure<sup>(2)</sup>.

#### 4. TEST PROCEDURES

Each specimen was placed in the testing machine with the web of the longitudinal horizontal and flange vertical. The axis of pull through the pins was made coincident with the centerline of the testing machine for the tests of all specimens.

For the room temperature tests, a preload of 160 kips was applied to the specimens to remove backlash in the fixture connections and to check over-all specimen alignment. Fourteen specimens were tested at room temperature to obtain elastic strain data. The indicated strains were measured for loads of 40, 80, 120 and 160 kips. The laboratory setup for the room temperature test of specimen 11A is shown in Figure 5.

For the tests to failure, the specimens were cooled to the temperature level selected for the particular test. Figure 6 shows the setup for a low temperature test. Strain readings were taken on gage elements parallel to the line of

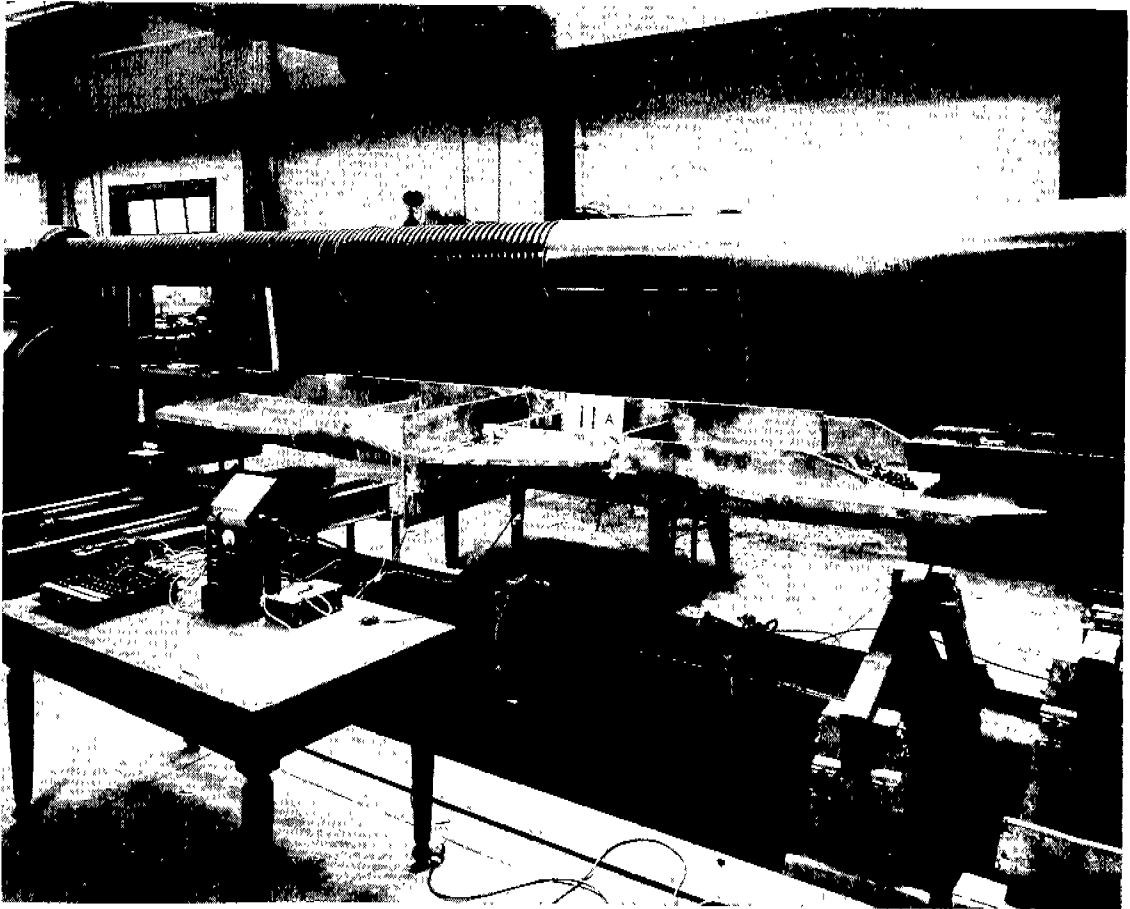


Fig. 5. Laboratory setup for room temperature test of specimen 11A.

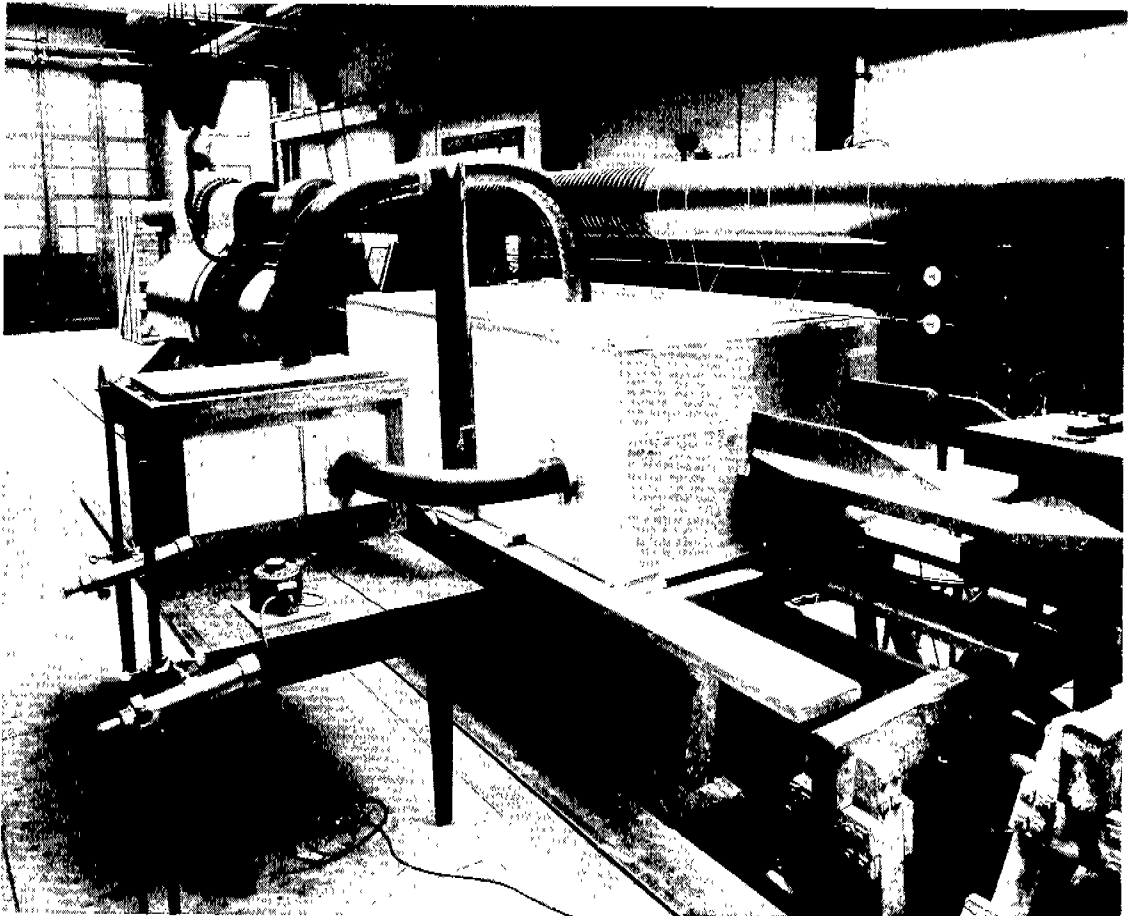


Fig. 6. Laboratory setup for a low temperature test to failure.

pull at load increments of 50 kips up to a load of 200 kips and thereafter at increments of 100 kips until failure was imminent. Dial extensometer and thermocouple readings were taken up to the instant of failure.

## 5. CALCULATIONS

The strains for corresponding gage elements on opposite sides of the plates were averaged for each load. The load-average strain data taken during the elastic tests at room temperature were extrapolated graphically to zero load to obtain the total indicated strains due to a load of 160 kips. The load-strain relationships for each gage location were reasonably well represented by straight lines.

The magnitude and direction of the principal stresses were computed by standard methods<sup>(4,5)</sup> from the linear load-strain relations for each rosette using values for Young's modulus of 30,100,000 lb. per sq. in. and Poisson's ratio of 0.290. Stresses in the axial direction were computed from the principal stresses. Stresses at plate edges on which gages were located were computed from the indicated strains and Young's modulus. Ratios of the computed axial stresses to the average stress in the longitudinal outside the region of the intersection were computed to give a measure of stress concentrations. The average stress in the longitudinal (P/A) was taken as the load, 160 kips, divided

by the measured area of the flanged longitudinal and bottom plate indicated in Figure 2 as section D-D on all specimens.

The average axial stresses on various components were computed and multiplied by the applicable cross sectional areas to determine the loads carried by the components and to compare total computed loads on specific cross sections with the machine load of 160 kips.

Energy to fracture values were determined from the load-extension relationships by numerical integration of the curve of load vs. elongation. To facilitate direct comparisons of energy to fracture, the computed values of energy were reduced to a common base. That is, for each specimen the computed value of energy was multiplied by the ratio  $\frac{25.48}{\text{Measured area at sect.D-D}}$ . The nominal area at section D-D for the interrupted longitudinal specimens was 25.48 sq. in.

## 6. RESULTS OF TESTS AT ROOM TEMPERATURE

### 6.1 Elastic Test of a Through Longitudinal

The elastic data taken during the test of through longitudinal specimen OA indicated that serious stress raisers were eliminated in this specimen. Some results of the elastic test are given in Table 2. The axial direction of the principal stresses, shown in Figure 7, are one result of minimizing the local constraints and "hardspots" of stress. Axial stresses computed from the principal stresses on the bottom plate and

Table 2 - Measurements and Results of Elastic Tests. Machine Load: 160,000 lb

	Specimen No.													
	Thru Long'l	Interrupted Longitudinals										Thru Bracket Long'ls		
	OA	1A	1A2	1A3	10A	11A	2A	2A3	3A	12A	13A	13A2	14A	15A
Test temperature, °F	90	74	81	85	80	76	83	83	73	79	79	81	72	73
<b>Section thru the Long'l</b>														
Area, in <sup>2</sup>	18.84	25.06	25.63	25.48	25.89	25.42	25.58	25.88	25.60	25.61	21.14	20.99	21.04	20.89
Average stress, lb/in <sup>2</sup> x 10 <sup>-3</sup>	8.50	6.39	6.24	6.28	6.18	6.29	6.26	6.18	6.25	6.25	7.57	7.62	7.60	7.66
Max. stress* ratio in bottom plate	1.0	1.1	-	-	-	-	0.8	-	0.8	-	1.2	1.3	0.8	1.1
Max. stress* ratio in longitudinal	1.4	2.1	-	-	-	-	2.2	-	2.0	-	1.9	2.1	1.8	1.6
Bottom plate load, lb x 10 <sup>-3</sup>	61.5	63.0	-	-	-	-	58.5	-	63.0	-	55.0	-	51.6	56.3
Longitudinal load, lb x 10 <sup>-3</sup>	101.3	95.8	-	-	-	-	100.8	-	96.6	-	98.8	-	92.7	100.4
<b>Section B-B</b>														
Area of bottom plate, in <sup>2</sup>	7.90	13.57	13.50	13.60	13.44	13.52	13.45	13.40	13.55	19.56	9.80	9.72	9.74	9.76
Bottom plate load, lb x 10 <sup>-3</sup>	59.4	101.9	-	-	96.8	-	100.4	-	97.9	103.8	63.2	65.7	59.4	68.0
Max. stress* ratio in bottom plate	1.1	1.4	1.4	1.6	1.4	1.5	1.5	1.5	1.3	1.0	1.4	1.1	1.1	1.3
Area of bracket, in <sup>2</sup>	10.90 <sup>+</sup>	13.60	13.45	13.37	13.57	13.47	13.47	13.30	13.52	13.53	11.83	11.52	11.72	12.98
Bracket load, lb x 10 <sup>-3</sup>	98.2 <sup>+</sup>	56.7	-	-	60.8	56.7	62.3	-	60.9	53.3	94.7	101.0	86.0	95.2
Max. stress* ratio in bracket	1.2 <sup>+</sup>	2.3	2.5	2.4	2.3	2.5	2.7	2.8	2.1	2.1	1.6	1.9	1.4	2.3
<b>Section C-C</b>														
Bottom plate load, lb x 10 <sup>-3</sup>	-	-	-	-	-	-	-	-	-	-	64.9	71.2	67.5	70.0
Max. stress* ratio in bottom plate	-	-	-	-	-	-	-	-	-	-	1.3	1.1	1.1	1.2
Freeing hole stress ratio	-	-	-	-	-	-	-	-	-	-	1.2	1.3	1.2	2.1

\* Stresses given are for the axial direction.

+ Values for flanged longitudinal near intersection with transverse bulkhead.

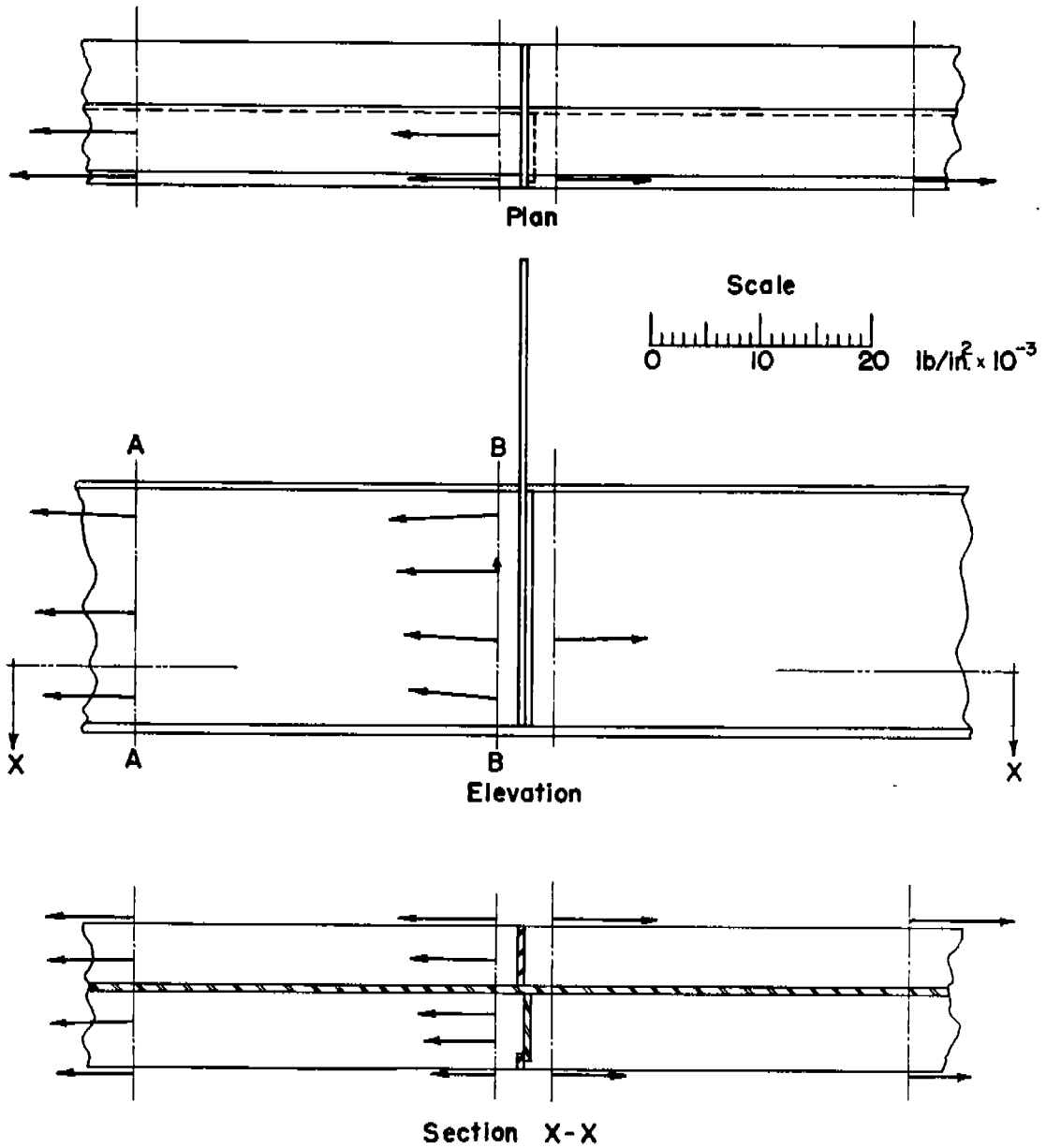


Fig. 7. Specimen OA, principal stresses at 160 kips load. Minor principal stresses less than  $1.0 \text{ kip/in.}^2$  not shown.

longitudinal adjacent to the transverse bulkhead are shown in Figure 8. Axial stress ratios on this section ranged from 0.7 to 1.2.

### 6.2 Elastic Tests of Nine Interrupted Longitudinals

Tests at room temperature were made on nine interrupted longitudinal specimens to obtain information on their elastic behavior. Some results of these tests are given in Table 2. Extensive strain data were taken on three interrupted longitudinals. These were specimens representing the original design in T-2 tankers (1A) and the two major modifications of this longitudinal in service (2A and 3A). Strain gage data taken on six other specimens were limited to checking results of previous tests and studying effects of minor modifications made in a particular design.

The magnitude and direction of the principal stresses for the three designs of interrupted longitudinals are shown in Figure 9. Comparisons of these stresses and their directions indicate that somewhat similar stress patterns were obtained for the brackets, bottom plates and longitudinals of the different specimens. The major principal stresses in the bracket were directed toward the flange of the longitudinal. Convergence of the major principal stresses in the bottom plates was toward the web of the longitudinals, while in the longitudinal web, the convergence was toward the line

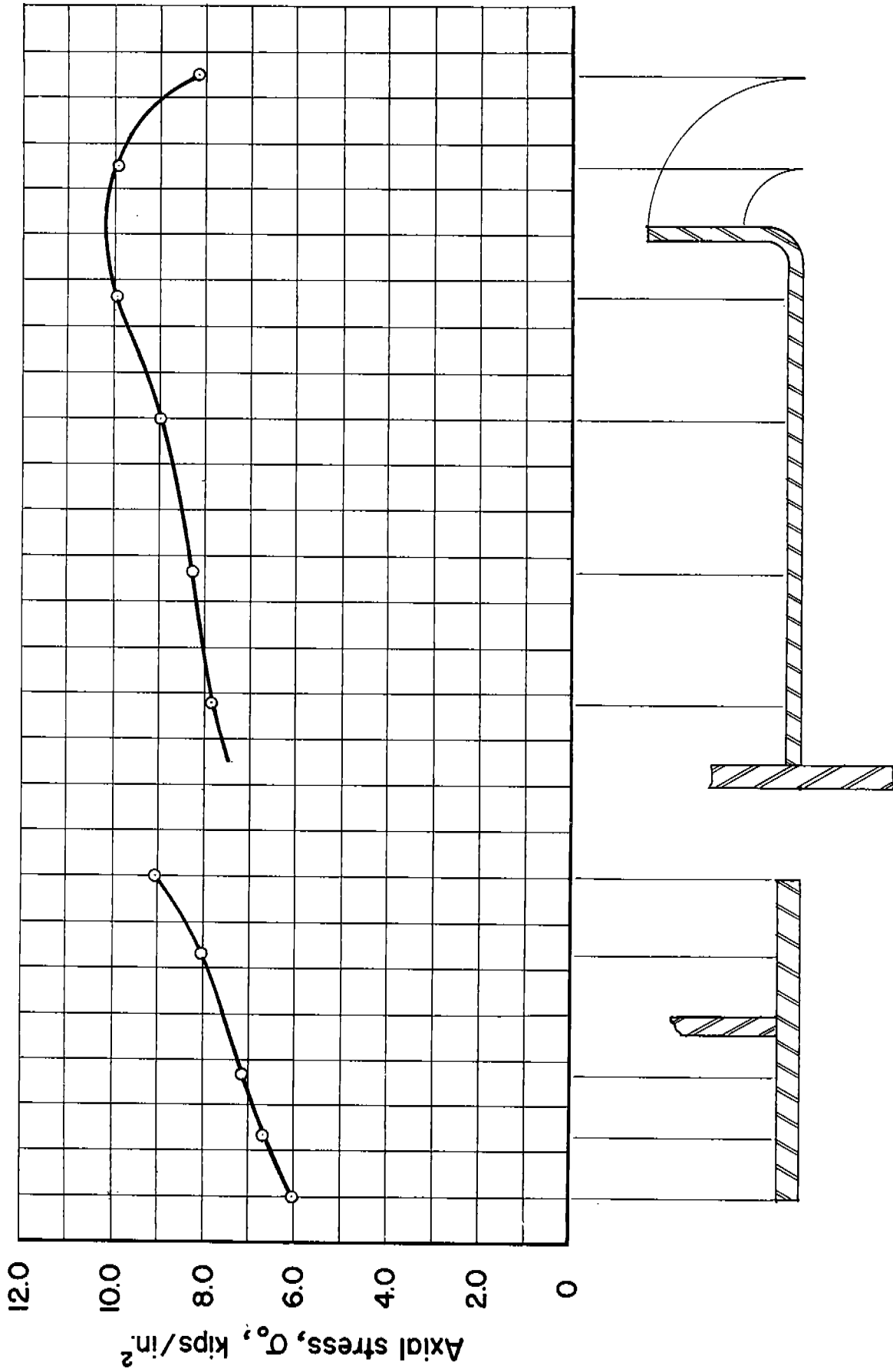


Fig. 8. Specimen OA, axial stresses on the bottom plate and longitudinal adjacent to the transverse bulkhead.

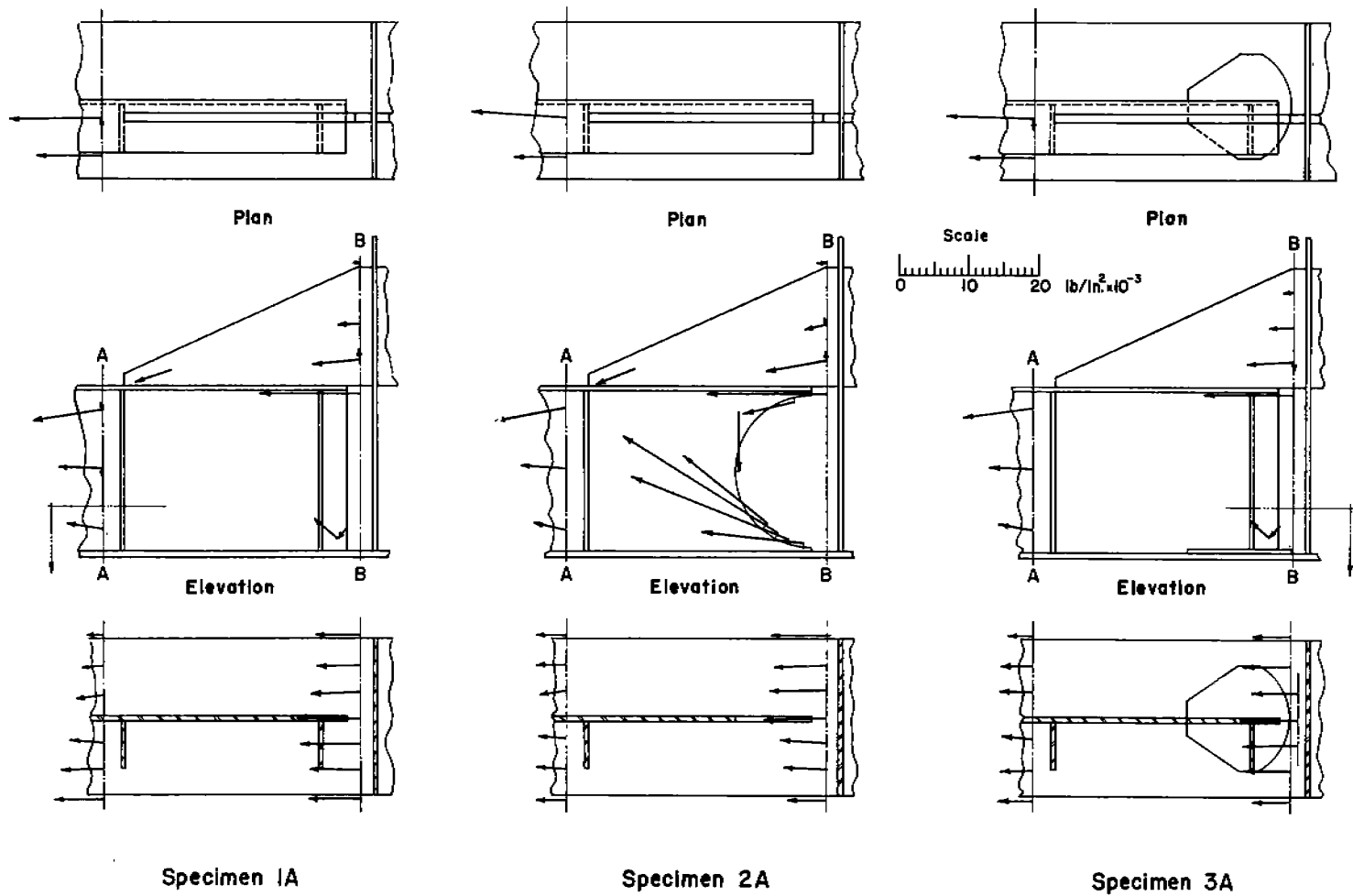


Fig. 9. Specimens 1A, 2A and 3A, principal stresses at 160 kips load. Minor principal stresses less than  $1.0 \text{ kip/in.}^2$  not known.

of pull.

The stresses measured on the edge of the semi-circular cutout of specimen 2A were about five times as large as the major principal stresses in similar locations on specimens 1A and 3A. The higher principal stresses were measured in areas adjacent to mechanical notches on all specimens. The most pronounced stress raisers were (1) the ends of the longitudinal flanges at the underedge of the 40.8# bracket, (2) the ends of the web of the longitudinals in the bottom plate and (3) the tapered ends of the bracket in the flange of the longitudinals. The notch formed by the longitudinal web and the bottom plate has been a source of major ship casualties. The other stress raisers could be contributing factors.

The axial stress distributions on the bottom plates and longitudinals, section A-A, were computed for specimens 1A, 2A and 3A. These distributions, figure 10, show the effects of the tapered end of the 40.8# bracket as a stress raiser. The axial stress ratios at these locations in the longitudinal flanges ranged from 2.0 to 2.2. Maximum bottom plate stress ratios varied from 0.8 to 1.1. No marked change of stress in this section was observed where the longitudinal web joined the bottom plate.

Representative axial stress distributions computed for the bottom plates and brackets, section B-B, are given in

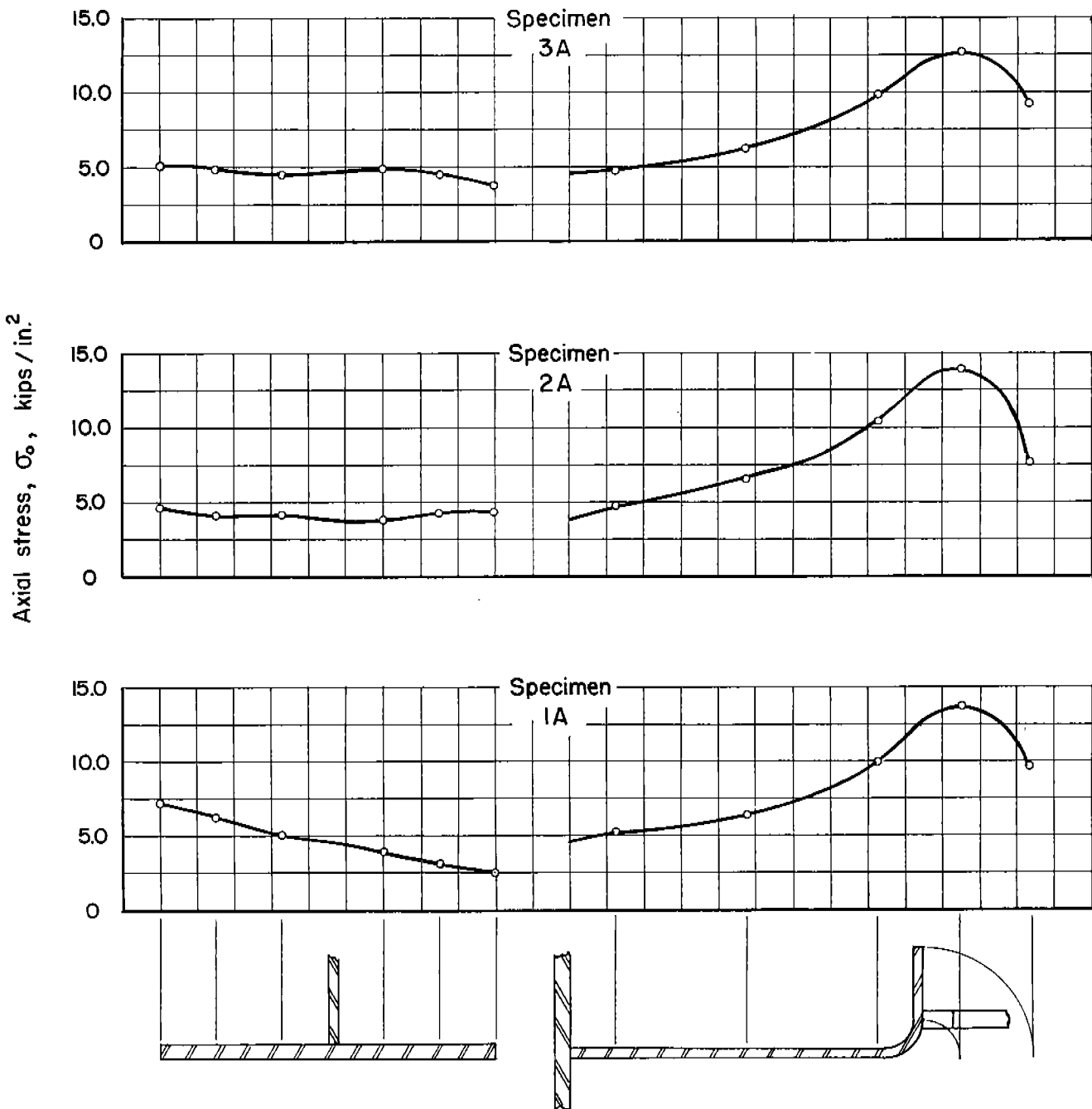
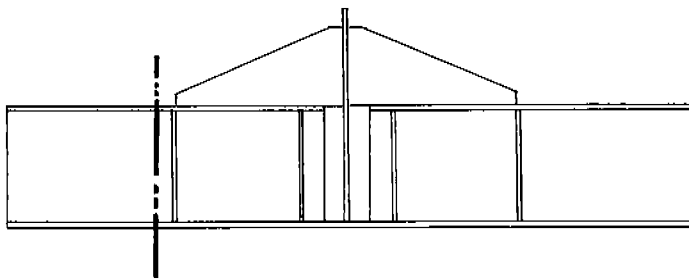


Fig. 10. Axial stress distribution on the bottom plate and longitudinal, section A-A, of specimens 1A, 2A and 3A.

Figure 11 for a load of 160 kips. The peak values of stress measured on the bottom plates were in line with the longitudinal webs. The maximum stress ratios measured on the bottom plates of nine interrupted longitudinals ranged from 1.0 to 1.6. Stress concentrations on the bottom plates were smaller for those specimens with doubler plates in the area of the stress raisers. The highest values of stress on the brackets were measured at the ends of the longitudinals as shown in Figure 11. The axial stress ratios at these points ranged from 2.1 on the more rigid specimens, 3A and 12A, to 2.8 on the more flexible 2A specimens. The maximum stress ratios on the brackets of the 1A specimens of intermediate rigidity were from 2.3 to 2.5. Except for specimen 3A, small compressive stresses were measured on the upper edge of the bracket of all interrupted specimens.

Some unbalance or gradient of stresses on the bottom plates was expected and observed due to gravity forces and minor misalignments inherent in the fabrication of large welded structures. These factors are thought to have had little significant effect on the results of these tests.

Sufficient strain data were taken on five interrupted specimens to compute the loads carried by the bottom plates and brackets of section B-B. The sums of these loads, Table 2, differed from the testing machine load of 160 kips by -1.8 to 1.7 per cent.

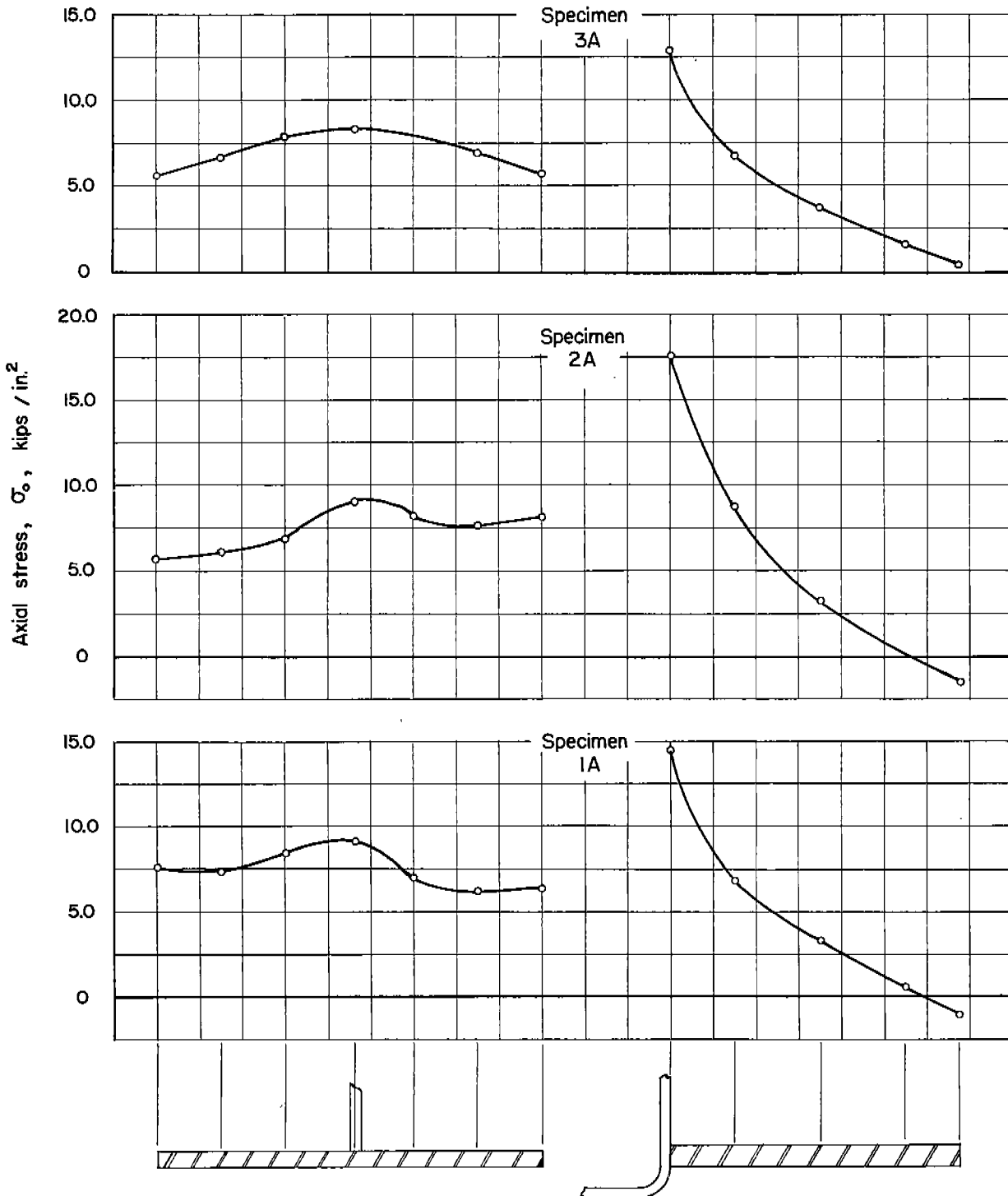
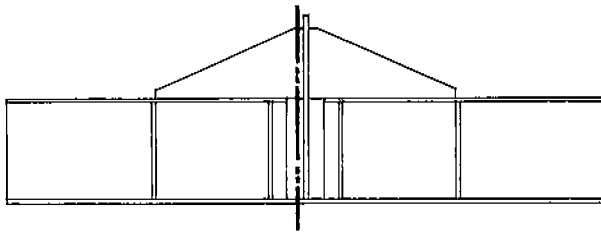


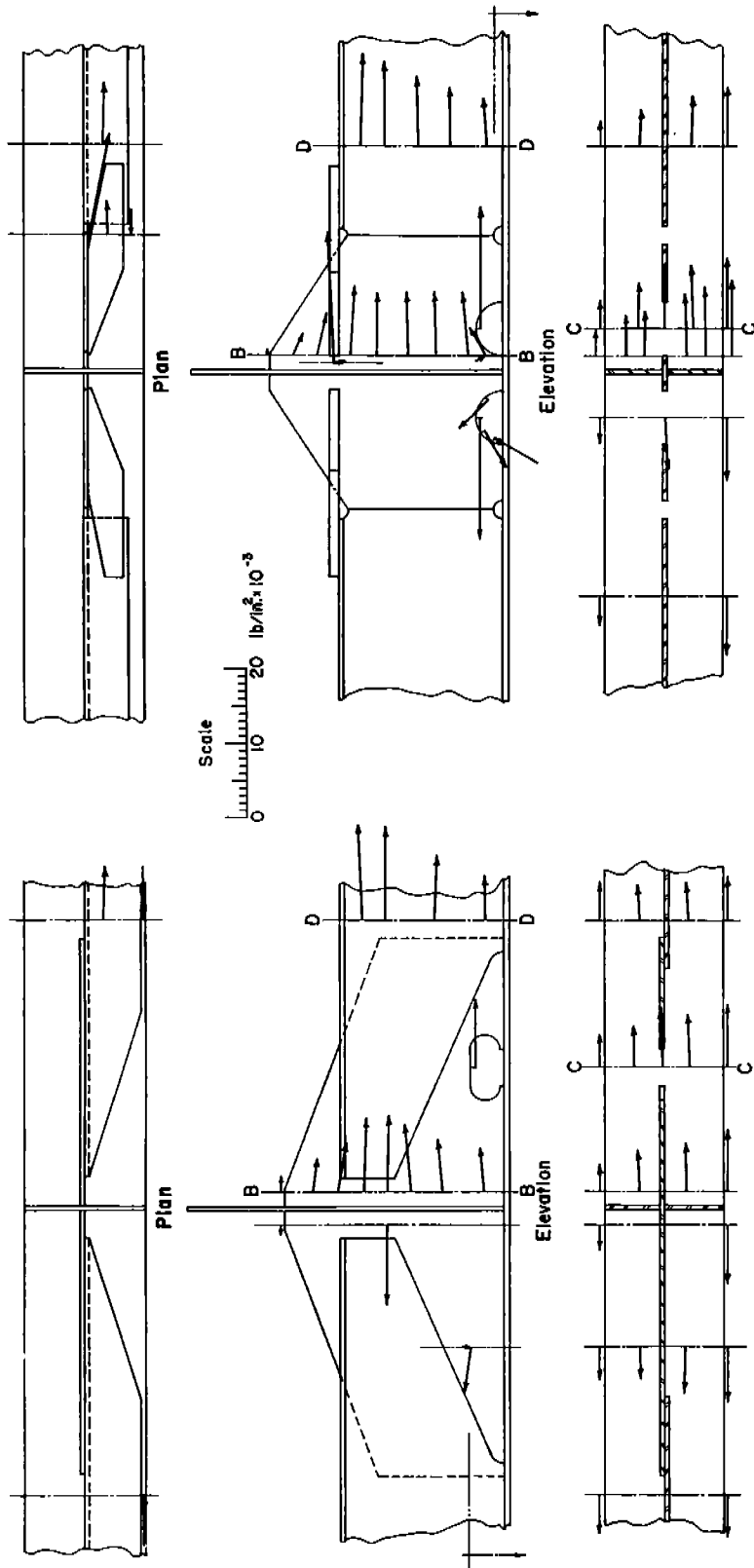
Fig. 11. Axial stress distribution on the bottom plate and bracket, section B-B, specimens 1A, 2A and 3A.

### 6.3 Elastic Tests of Four Through-Bracket Longitudinals

The four through-bracket longitudinal specimens were gaged and tested at room temperature for elastic stress distribution. Some results of these tests are given in Table 2.

The magnitude and direction of the principal stresses for a load of 160 kips are shown in Figure 12 for through-bracket longitudinal specimens 14A and 15A. The stress patterns found for specimens 13A and 13A2 were similar to the stress patterns for specimen 14A. Major principal stresses in the through-brackets, section B-B, were directed toward the central portion of the longitudinal web. The major principal stresses in the bottom plates were generally parallel to the line of pull. Stresses measured on the edges of the freeing holes in the longitudinal webs were large compared to stresses at nearby locations. Comparable stresses were indicated on a photoelastic model of specimen 13A studied in another laboratory<sup>(6)</sup>.

A pronounced stress gradient was present across the flat bar of specimen 15A approximately in line with the butt-weld joint. The major principal stresses in the longitudinals outside the intersection were generally axial and reached highest values in the longitudinal webs 2 to 3 inches below the root of the flange. Compressive stresses were measured



Specimen 15A

Specimen 14A

Fig. 12. Specimens 14A and 15A, principal stresses at 160 kips load. Minor principal stresses less than 1.0 kips/in.2 not shown.

on the edge of the flanges, section D-D, of the 13A specimens.

The axial stress distributions on the bottom plates and brackets, section B-B, of specimens 13A, 14A and 15A are shown in Figure 13. For a load of 160 kips, the maximum stresses on the bottom plates of through-bracket specimens were measured on the upper plate edges as referred to the position of the specimen in the testing machine. Maximum axial stress ratios ranged from 1.1 to 1.4 on section B-B across the bottom plates. Axial stresses on the brackets reached peak values in the 13A design near the end of the tapered lap-weld joint of the longitudinal web and through-bracket about twelve inches above the inside of the bottom plate. The highest axial stress measured on specimen 15A was found on the through-bracket at the end of and in line with the 40.8# flat bar. Stress concentrations of 1.4 to 1.9 were found on the through-brackets of the 13A design, and a maximum concentration of 2.3 was found for specimen 15A.

The effects of the freeing holes on the stress distribution on the bottom plate section C-C are shown in Figure 14. An increase of stress on the bottom plates in line with the web of the longitudinals was noted. The axial stress ratios under the center of the freeing holes were from 1.0 to 1.1.

The axial stress distributions on the bottom plate and longitudinal, section D-D, were computed for the through-bracket specimens and are shown in Figure 15 for specimens

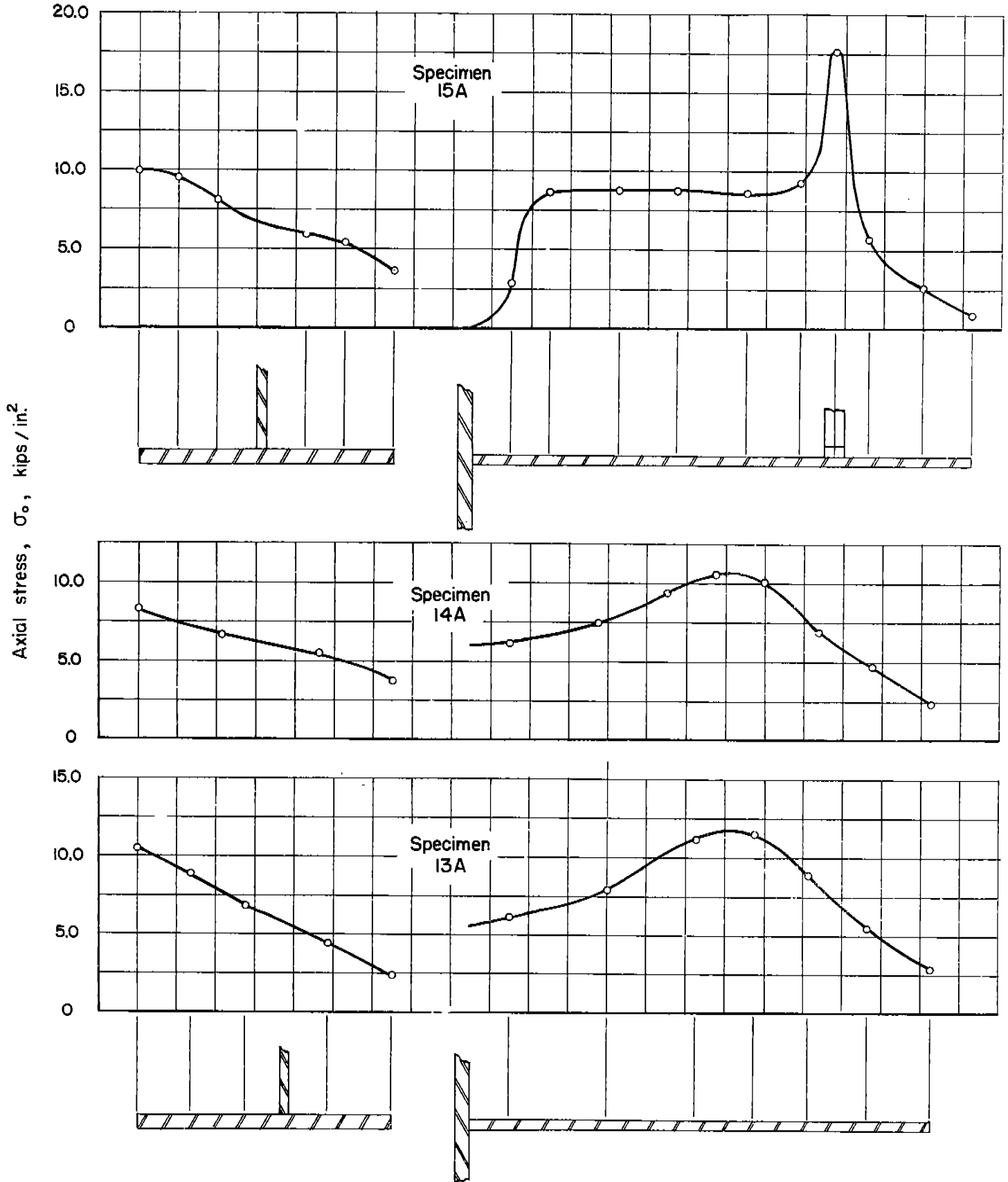


Fig. 13. Axial stress distribution on bottom plate and through-bracket, section B-B, specimens 13A, 14A and 15A.

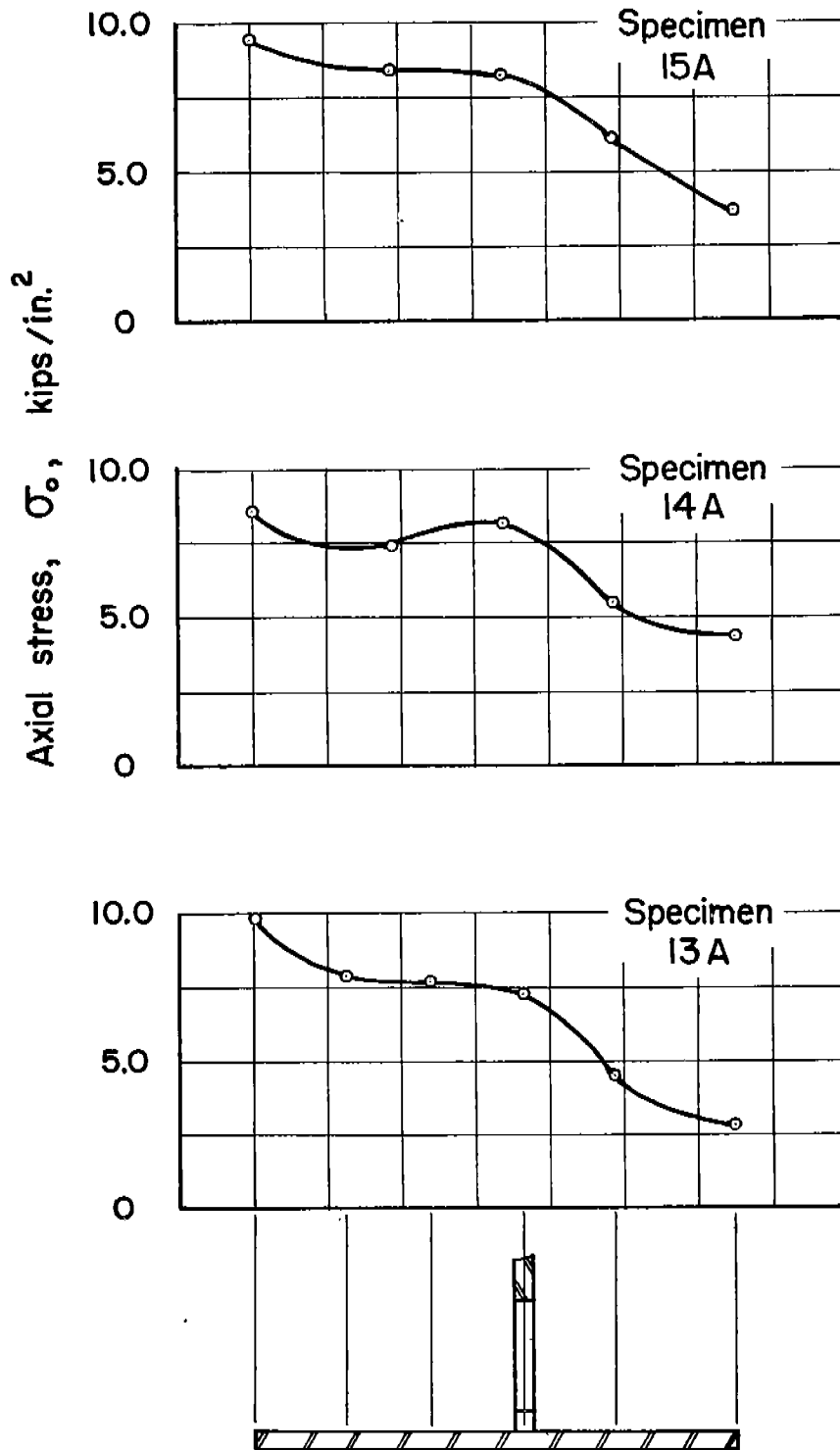


Fig. 14. Axial stress distribution on bottom plate, section C-C, specimens 13A, 14A and 15A.

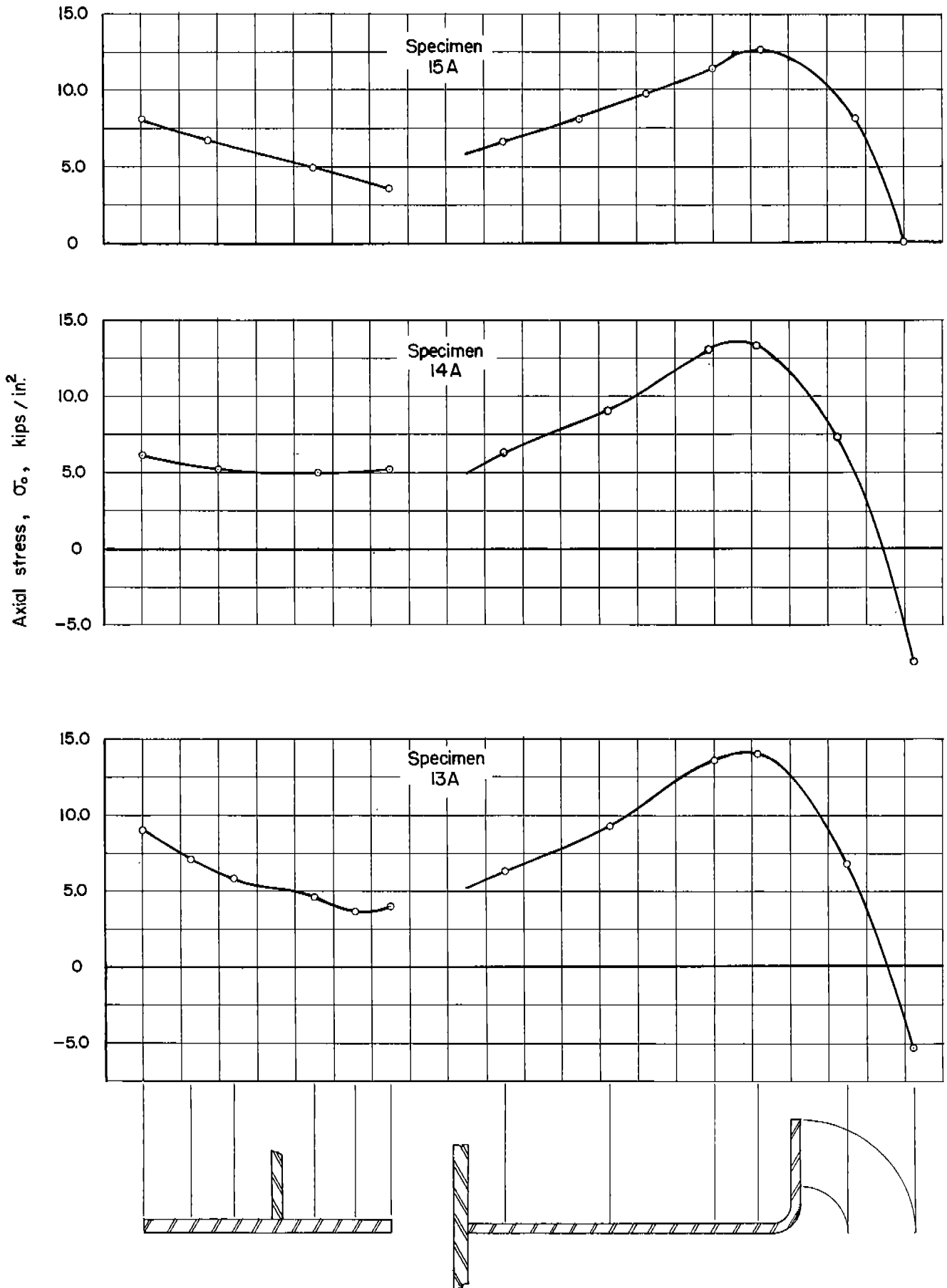


Fig. 15. Axial stress distribution on bottom plate and longitudinal, section D-D, specimens 13A, 14A and 15A.

13A, 14A, and 15A. Bottom plate stresses were higher on the upper edge of the plate except on 13A2, which was misaligned with the pulling heads. Maximum stress ratios on section D-D of the bottom plate ranged from 0.8 to 1.3. Stress concentrations ranging from 1.6 to 2.1 were found in the web of the longitudinal 2 to 3 inches below the root of the flange.

Gravity forces acting on the through-bracket specimens caused stresses on the upper edge of the bottom plates to be considerably larger (excluding specimen 13A2) than stresses on the lower edge. Initially, the specimens were deflected downward under the action of gravity forces such that the straightening which accompanied the axial loads caused the axial and bending stresses to be additive on the upper edge of the plates.

The loads carried by the bottom plates and brackets of section B-B were computed from the average axial stresses and areas of the respective components. These and other loads computed similarly are listed in Table 2. The sums of the bottom plate and bracket loads for the through-bracket longitudinals differed from the testing machine loads, 160 kips, by -9.1 to 4.2 per cent.

## 7. RESULTS OF LOW TEMPERATURE TESTS

### 7.1 Test to Failure of a Through Longitudinal

With the temperature at  $-4^{\circ}\text{F}$ , through longitudinal

specimen OA failed with cleavage fractures across the longitudinal and bottom plate (Figure 16) after sustaining a load of 1,113 kips. Chevron patterns on the fracture surfaces and the position of the specimen after failure relative to the line of pull indicated that the origin of the fracture was at the root of the formed flange. The measured reduction of area of the fractured section was 6 per cent. Some results of the low temperature tests are given in Table 3.

Selected axial strain gages on specimen OA were read at load up to 700 kips. The strain distributions on section B-B as determined from the average axial strains for several loads are shown in Figure 17. At a load of 700 kips the strains measured on the bottom plate and longitudinal at this section adjacent to the transverse bulkhead ranged from 0.11 to 0.57 per cent. Strain gradients on section B-B did not appear excessive for this load and type of specimen.

The energy to fracture as computed from the load versus the centerline extension relation was 342,200 ft-lb. Assuming other factors vary proportionately to changes in area, if the calculated energy to fracture specimen OA is adjusted to compare with the energy of a geometrically similar specimen with the nominal area of the interrupted longitudinals outside the intersection, the energy to fracture would be 462,800 ft-lb.

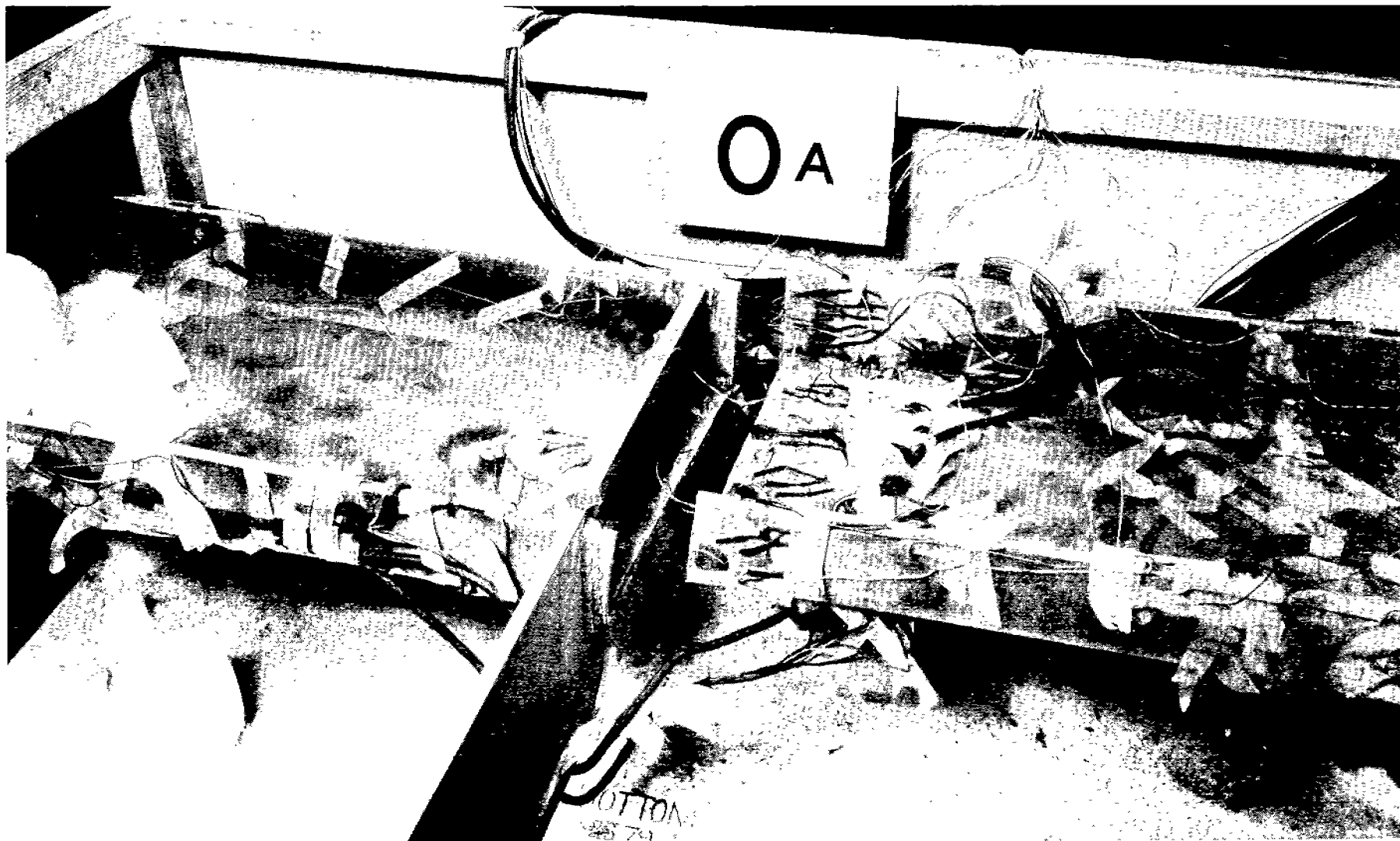


Fig. 16. Specimen OA immediately after fracture. Maximum load 1,113 kips.

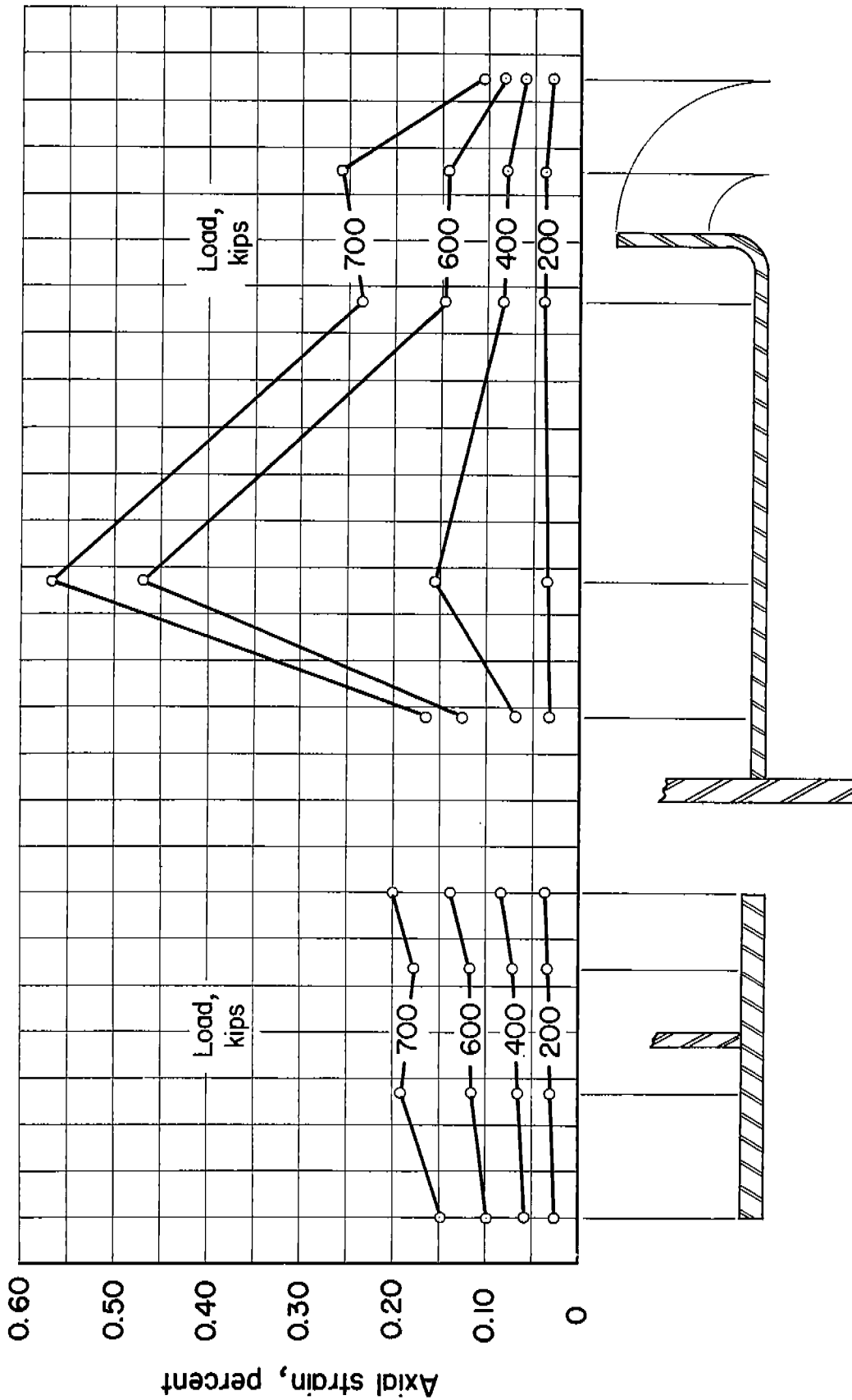


Fig. 17. Axial strain distribution on the bottom plate and longitudinal, section B-B, of specimen OA.

Table 3. Results of Low Temperature Tests

Specimen No.	Test Temp. °F	Max. Load kips	Avg. Stress on Long'l, Sect. D-D, at Failure kips/in. <sup>2</sup>	Axial Extension in.	Energy to Fracture ft-lb	Adjusted Energy to Fracture ft-lb
Thru Longitudinal						
0A	-4	1,113	59.1	4.48	342,200	462,800
Interrupted Longitudinals						
1A	-13	843	33.6	0.52	28,300	28,800
1A2*	38	1,083	42.3	1.39	102,900	102,300
1A3	21	1,015	39.8	0.91	62,700	62,700
1A4	-6	905	35.3	0.62	36,300	36,100
1A5	3	1,052	41.1	1.31	94,100	93,600
1A6	-1	831	31.6	0.48	24,900	24,100
10A	-2	960	37.1	1.00	64,300	63,300
11A	-7	912	35.9	0.62	36,000	36,100
2A*	-1	993	38.8	1.71	121,600	121,100
2A2*	0	918	36.3	2.18	141,000	142,200
2A3	-20	826	31.9	0.23	11,300	11,100
2A4	-2	981	38.1	1.18	78,700	77,800
3A	8	1,091	42.6	1.68	126,300	125,700
12A*	-4	1,047	40.9	0.92	65,900	65,600
Thru-Bracket Longitudinals						
13A*	-2	938	44.4	1.37	88,900	107,200
13A2*	2	834	39.7	0.42	21,000	25,500
14A	0	1,144	54.4	2.24	172,500	208,900
15A	3	799	38.2	0.57	30,200	36,800

\* Specimen failed outside the intersection.

### 7.2 Tests to Failure of Fourteen Interrupted Longitudinals

Ten of the interrupted longitudinal specimens were tested to failure at temperatures ranging from  $-7^{\circ}$  to  $8^{\circ}$ F. Two interrupted longitudinals were tested at temperatures somewhat higher than  $0^{\circ}$ F and two somewhat lower to obtain information on the effects of temperature on the mode of fracture. Some results of the tests to failure of fourteen interrupted longitudinals are summarized in Table 3.

The maximum loads, listed in Table 3, sustained by the interrupted longitudinals before failing were from 826 to 1,091 kips. The surfaces of the fractures were granular in appearance. Ten specimens failed with fractures across the bottom plate and bracket adjacent to the transverse bulkhead and four specimens failed in the longitudinal outside the intersection. Specimen 10A immediately after fracture is shown in Figure 18. The chevron pattern on the fracture surfaces and the position of the specimen after failure indicated that, in the ten specimens which fractured through the intersection, the fractures originated in the center of the bottom plate at the end of the longitudinal web, except for specimen 2A3. In this specimen, the origin of the initial fracture appeared to be at the under edge of the bracket at the end of the longitudinal flange. The origin of fracture in the four interrupted specimens that failed outside the intersection was at the root

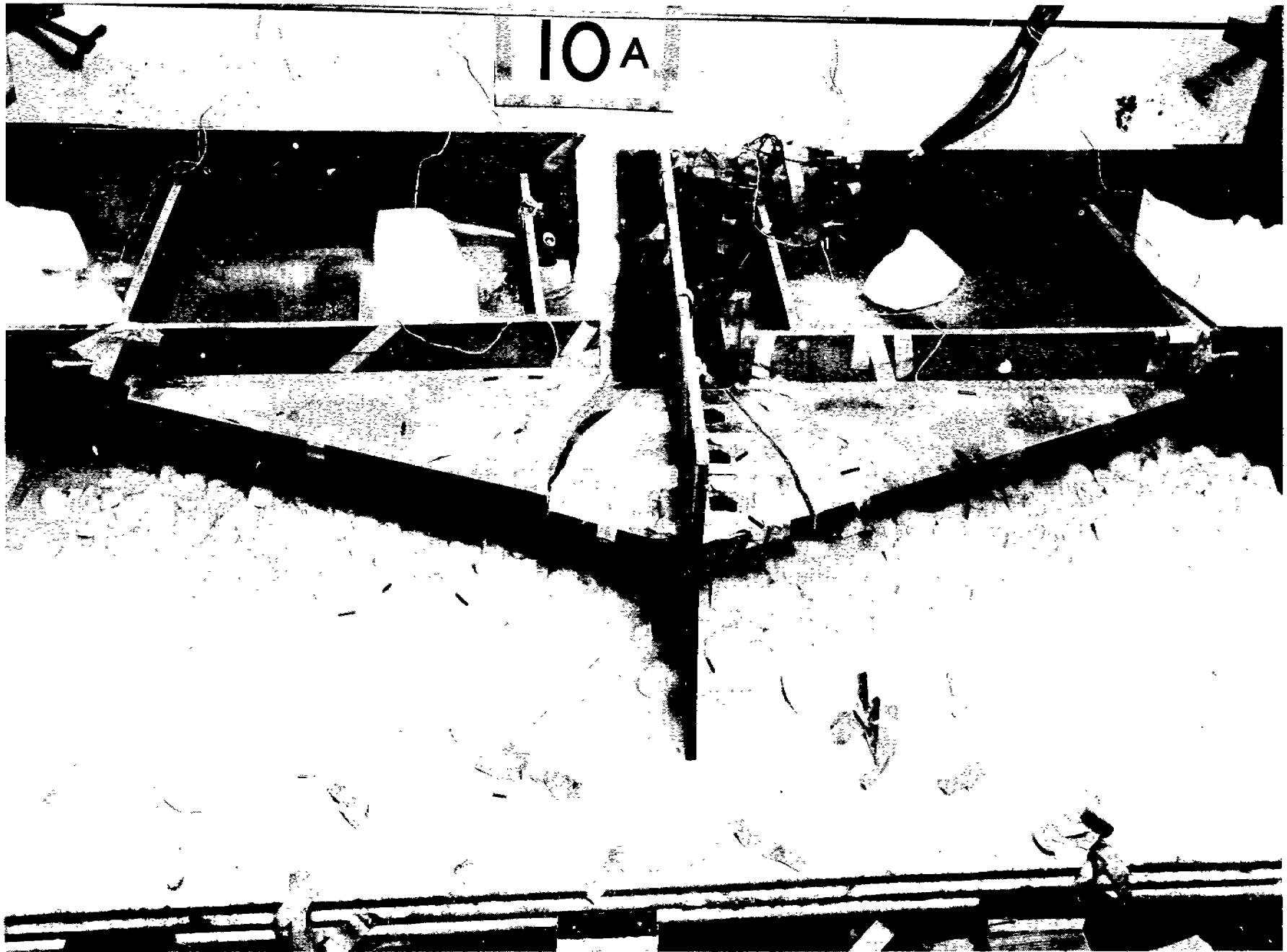


Fig. 13. Specimen 10A immediately after fracture.  
Maximum load: 960 kips.

of the flange adjacent to the pulling head (specimens 1A2, 2A and 12A) and in the longitudinal flange at one end of the bracket (specimen 2A2).

At the edge of the fracture of specimen 3A, in the center of the bottom plate, a reduction of plate thickness of 4 per cent was measured. No appreciable reduction of plate thickness could be measured with micrometer calipers at the fracture edges of other specimens.

Axial strain gages were read on all interrupted longitudinal specimens until failure appeared imminent. Strain distributions were determined for various sections of one or more of each design of interrupted longitudinal. The axial strain distributions on section A-A of specimens 1A, 2A and 3A are shown for several loads in Figure 19. The strain distributions measured on this section of the bottom plates were relatively even and did not exceed 0.12 per cent at 800 kips. Up to a load of 700 kips the axial strains on the longitudinal, section A-A, tended to peak at the end of the 40.8# bracket with values of strain from 0.65 to 0.84 per cent. At higher loads, the largest strains were measured on the edge of the flange. This is shown in the strain distribution curves for specimens 2A and 3A in Figure 19 at 800 kips load. The strains on the edges of the flanges were 1.86 and 2.18 per cent, respectively.

The axial strain distributions measured on the bottom plate and bracket, section B-B, of specimens 1A, 10A, 2A, 2A<sup>4</sup> and 3A

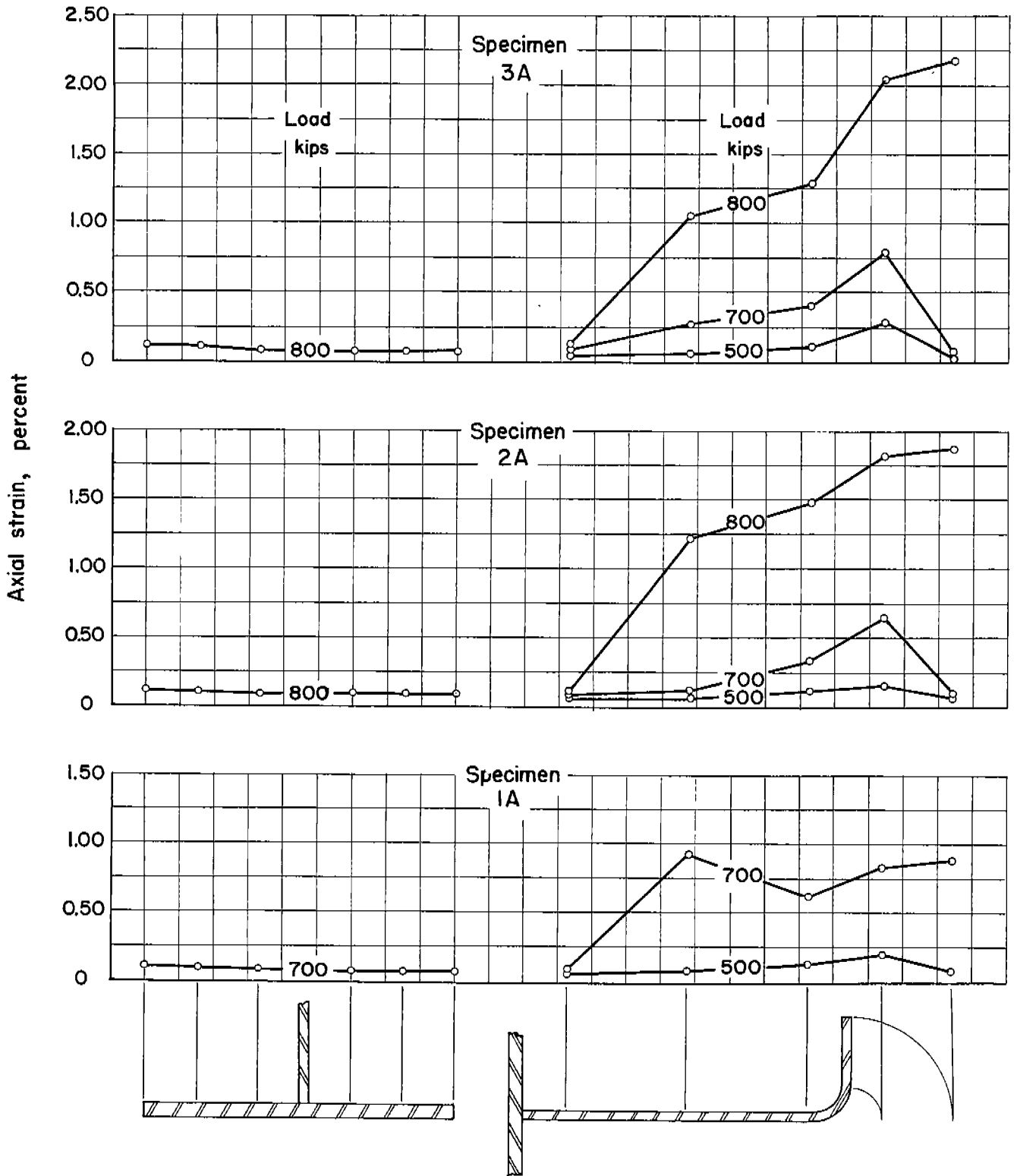


Fig. 19. Axial strain distribution on the bottom plate and longitudinal, section A-A, of specimens 1A, 2A and 3A.

are shown in Figure 20 for several loads. These curves are typical of the strain distributions measured on this section of the interrupted longitudinals tested at low temperatures except on specimen 12A. The strains on the bottom plate, section B-B, of specimen 12A ranged from 0.07 to 0.12 per cent for a load of 800 kips with relatively little concentration in the center of the plate. On all other interrupted longitudinals, strains measured on the bottom plates at the end of the longitudinal webs indicated a pronounced stress concentration at this mechanical notch. Excluding specimens 2A2 and 12A, the axial strains measured at this point in line with the longitudinal web were from 0.35 to 0.88 per cent for a load of 700 kips and from 0.65 to 1.62 per cent at 800 kips. The strain gages located at this point on the bottom plate had become inoperative on about half the specimens before a load of 800 kips was reached. Results involving plastic deformation of specimen 2A2 are not thought to be comparable with results measured on other specimens because the material in the bottom plate of 2A2 appeared to be quite different from the material in the other specimens. These differences are discussed in detail in the Appendix. The continuous outside doubler on specimen 12A was the only design detail which appeared to influence patterns of strain distribution on the bottom plates significantly.

The axial strains measured on the brackets of the interrupted

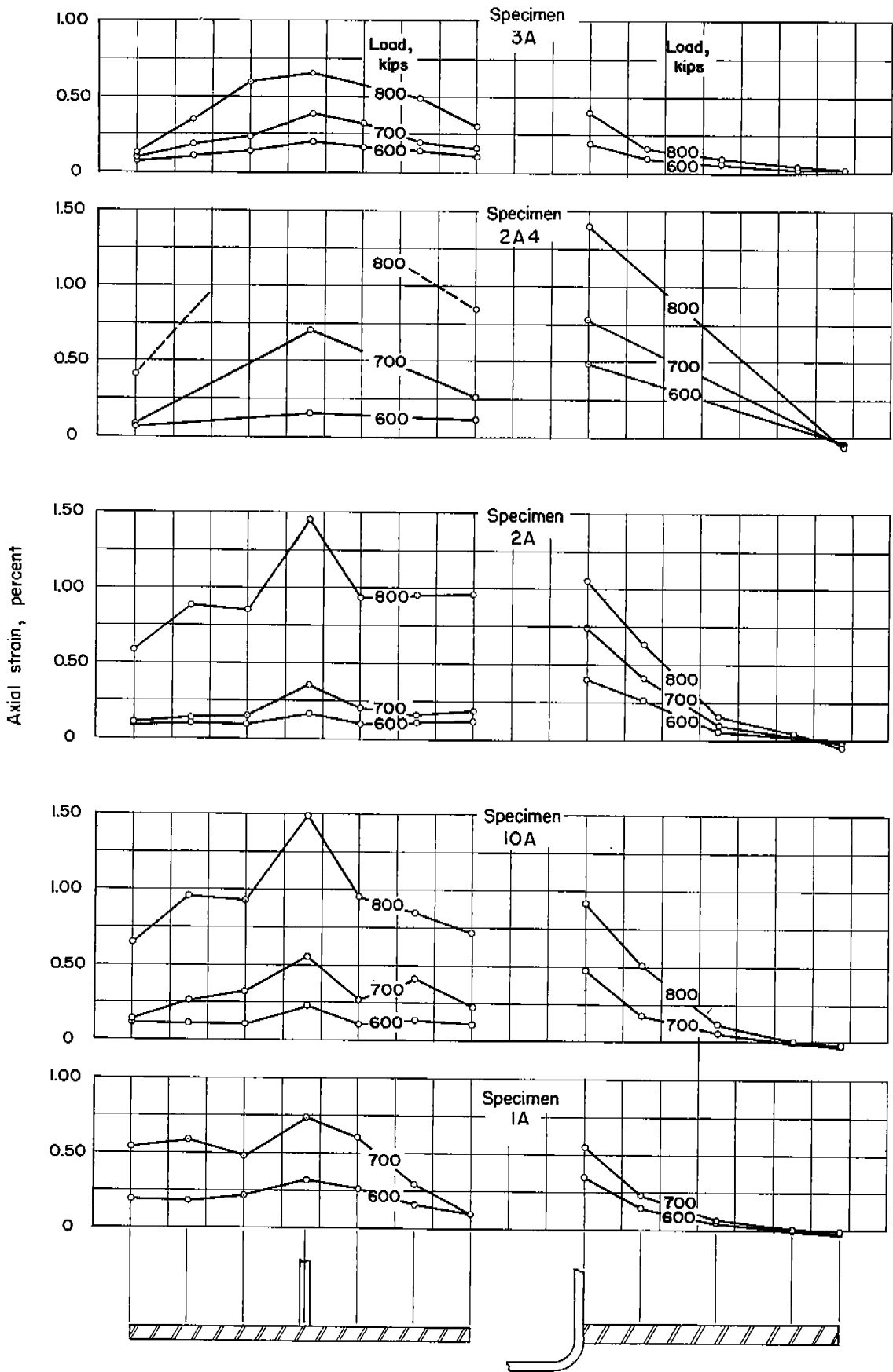


Fig. 20. Axial strain distributions on the bottom plate and bracket, section B-B, of specimens 1A, 10A, 2A, 2A4 and 3A.

longitudinals were influenced by the notch effect caused by terminating the longitudinal flange. Tensile strains in the plastic range were measured on the lower edges of the brackets at the end of the longitudinal flange and elastic strains, usually compressive, were measured on the upper edges. Excluding specimen 2A2 for reasons previously mentioned, the maximum strains were measured on the lower edge of the brackets and ranged from 0.24 to 0.78 per cent at 700 kips and 0.39 to 1.39 per cent at 800 kips. At 700 kips, the largest strains at this mechanical notch were measured on the somewhat flexible 2A specimens, intermediate values of strain were measured on the more rigid basic 1A specimens and the smallest strains were found on the most rigid 3A and 12A specimens. At 800 kips, the maximum strains measured on the 1A and 2A specimens did not differentiate clearly between the two designs. The strains on the lower edge of the brackets for 800 kips were from 0.90 to 1.26 per cent on the 1A specimens, from 1.06 to 1.39 per cent on the 2A specimens and 0.39 and 0.41 per cent on specimens 3A and 12A, respectively. Gages on three 1A specimens were inoperative at 800 kips.

Strains in the plastic range for the material were measured on the edge of the cutout in the longitudinal web of specimen 2A. At 700 kips, the magnitudes of these strains were 0.81 per cent on the edge near the bottom plate, -0.19 per cent in the center of the web, and 0.14 per cent on the edge adjacent to

the flange of the longitudinal. Strains measured at these points were 1.86, -0.24 and 0.20 per cent at 800 kips.

The energy required to fracture the interrupted specimens, listed in Table 3, was computed from the load versus centerline extension relationship for each specimen. The magnitudes of these energies were little changed when adjusted to be proportionate to the nominal area of the longitudinal outside the intersection. Excluding specimen 2A2, the adjusted energy values for nine specimens tested near 0°F ranged from 24,100 to 125,700 ft-lb. Comparison of the energies to fracture the specimens of the basic T-2 design or minor variations of it (specimens 1A4, 1A5, 1A6, 10A and 11A) with the more flexible (2A and 2A4) and the rigid specimens (3A and 12A) indicates that both methods of modifying the structure had improved the energy absorption ability when sustaining tensile loads.

Energy to fracture versus test temperature relationships were not definitely established from the results of these tests, but the general trend was apparent. When comparisons are restricted to specimens of one design, higher test temperatures were usually accompanied by higher energies to fracture. Within the small temperature range of -7° to 8°F, the energy to fracture values for nine interrupted longitudinals generally follow this trend as can be seen from inspection of Table 3. An exception was specimen 1A6 which failed at a low value of

energy compared with values for the other interrupted specimens. The following excerpts from Table 3 of values determined for four specimens tested at temperatures farther from 0°F show the influence of temperature on the energy to fracture these structures.

<u>Specimen No.</u>	<u>Test Temperature</u> degrees F	<u>Energy to Fracture</u> ft-lb
2A3	-20	11,100
1A	-13	28,800
1A3	+21	62,700
1A2	+38	102,300

Energy to fracture values versus test temperatures for eight specimens of the 1A design are shown in Figure 21. Test temperatures for these eight specimens ranged from -13° to 38°F. The trend for energy absorption to increase with higher temperature is apparent.

### 7.3 Tests to Failure of Four Through-Bracket Longitudinals

The results of tests to failure of four through-bracket longitudinals are given in Table 3. The fracture surfaces of these specimens, tested at or near 0°F were granular in appearance. Specimens 13A and 13A2 fractured through the longitudinal outside the intersection. The locations of these fractures were thought to result in part from an unsuitable design of the welded joints between the pulling heads and the longitudinal flanges. Remedial designs of this connection were

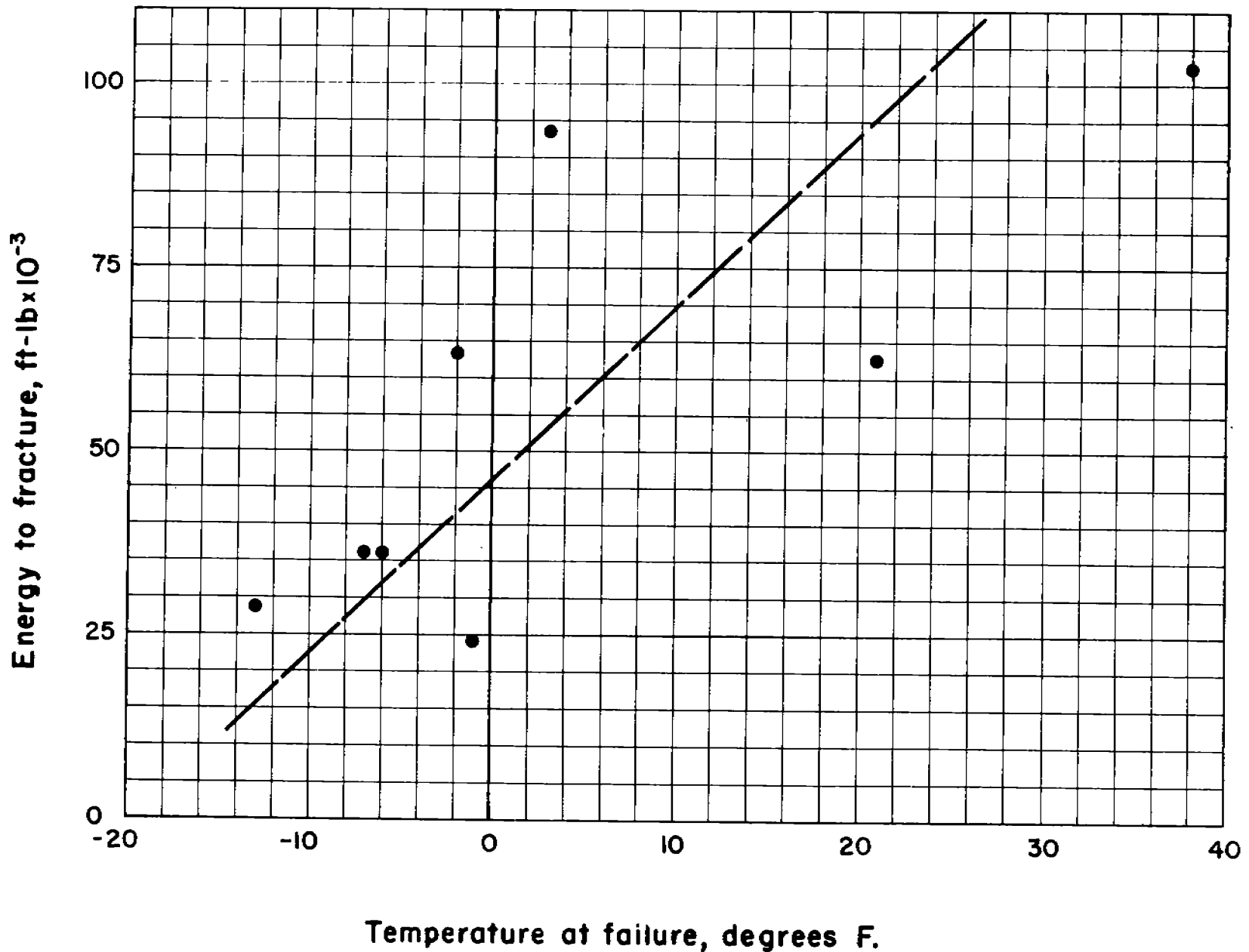
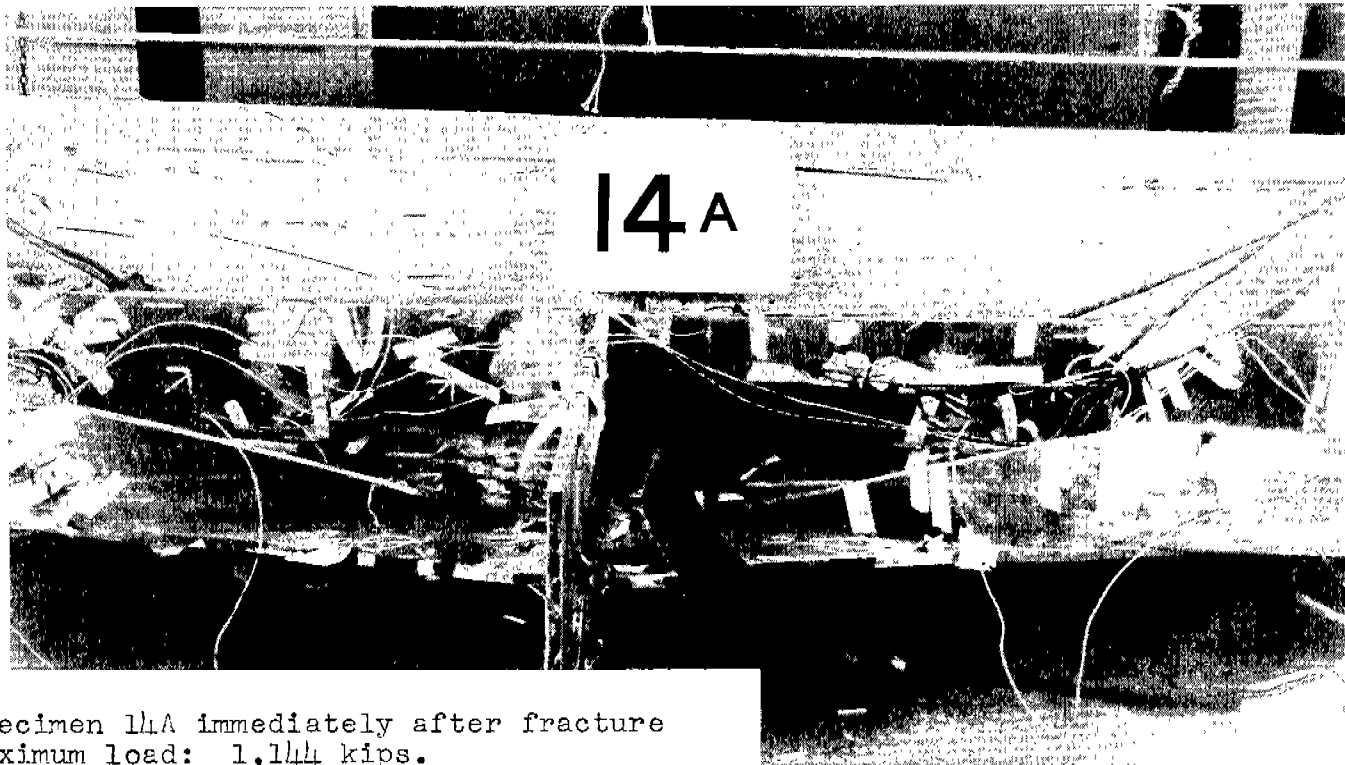


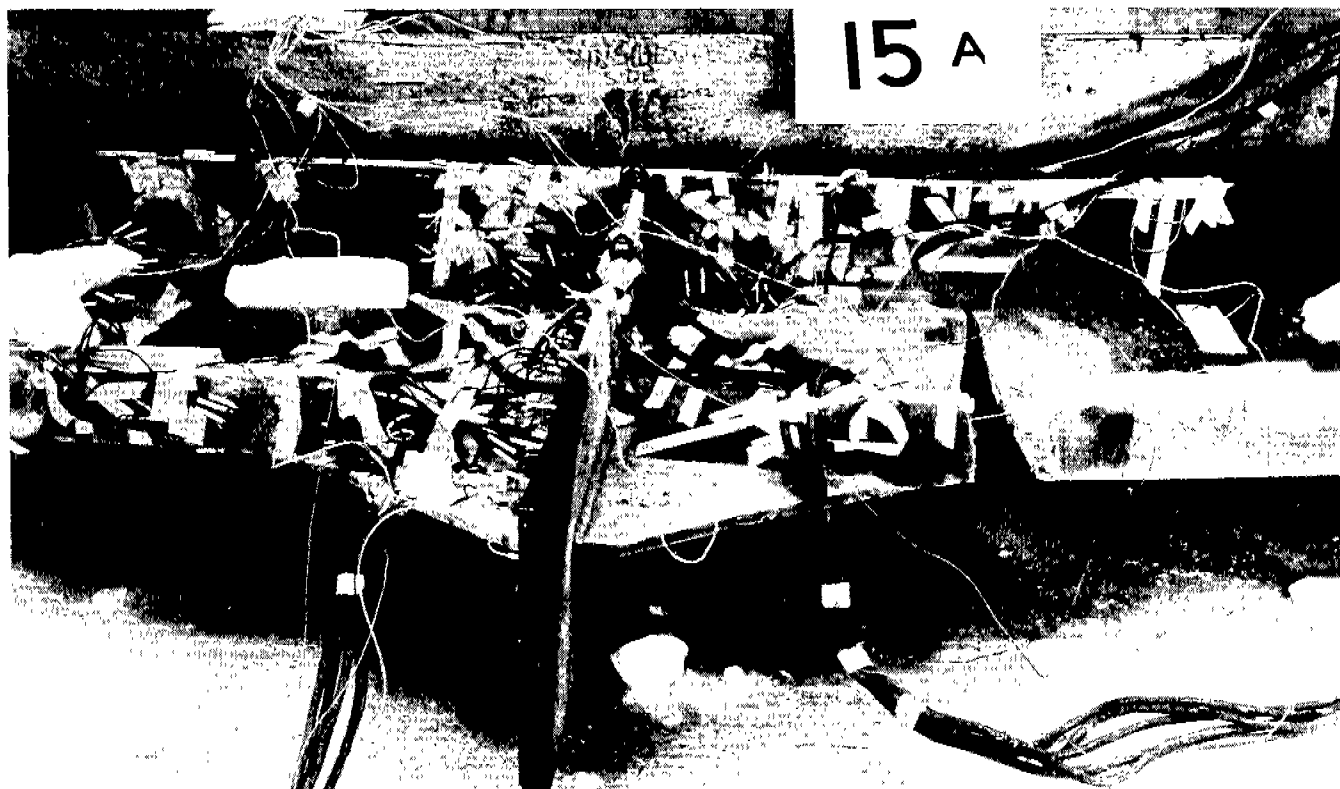
Fig. 21. Energy to fracture versus test temperature for eight interrupted specimens of 1A design. (Straight line fitted by the method of least squares).

incorporated in subsequent specimens. Inadvertently, specimen 13A2 was shortened 10 inches. This and the poor end connections probably invalidate direct comparisons of maximum load, axial extension and energy for this specimen with corresponding results measured on the other longitudinals. Specimens 14A and 15A sustained loads of 1,144 and 799 kips, respectively, before fracturing across the intersection. These specimens are shown in Figure 22 immediately after fracture. Examination of the chevron patterns on the fracture surfaces indicated that the fracture origin in specimen 14A was in the through-bracket at the end of the tapered longitudinal web, approximately 14 inches from the inside of the bottom plate. The fracture sources in specimen 15A appeared to be at the corner of the flat bar nearest the butt-weld joint and on the upper edge of the through-bracket adjacent to the butt-weld.

The axial strain gages at selected locations on various sections of the through-bracket longitudinals were read until failure appeared imminent. Strain distributions on various cross sections were determined from the average axial strains. The distribution of axial strains on the bottom plates and brackets of specimens 13A, 14A and 15A are shown for several loads in Figure 23. Maximum axial strains measured on the bottom plates, section B-B, of these three specimens ranged from 0.14 to 0.18 per cent at 600 kips, and from 0.25 to 0.36 per cent at 700 kips. Peaks of strain were developed due to



Specimen 14A immediately after fracture  
Maximum load: 1,144 kips.



Specimen 15A immediately after fracture.  
Maximum load: 799 kips

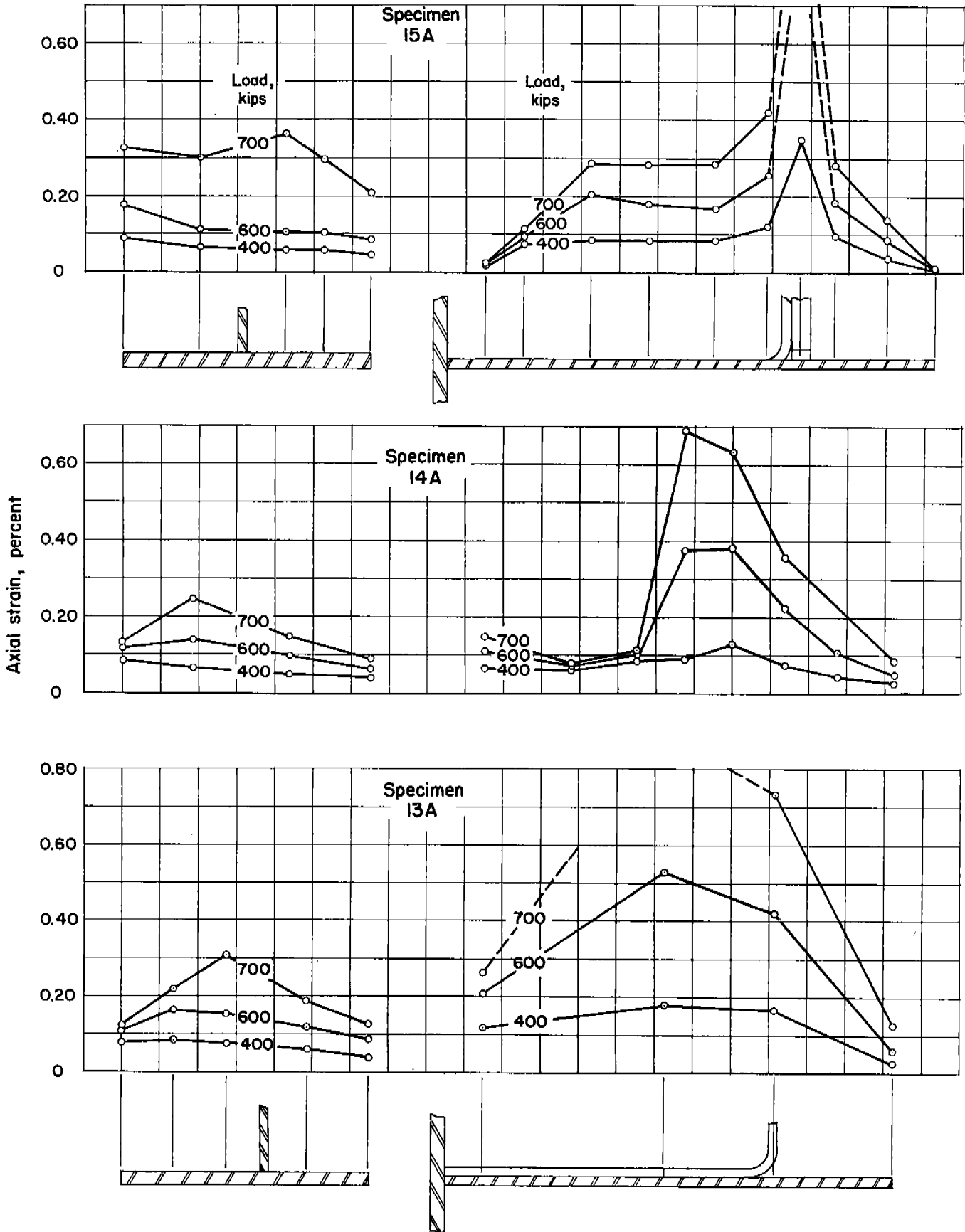


Fig. 23. Axial strain distributions on the bottom plate and bracket, section B-B, of specimens 13A, 14A and 15A.

localized plastic yielding on the bottom plate at 700 kips. The strain distributions on the through-brackets of specimens 13A, 14A and 15A reflected the effects of the freeing holes adjacent to the bottom plates and the mechanical notches caused by connecting the flanged longitudinals to the through-bracket. The peaks of strain were in the regions of maximum stress as determined in elastic tests. At 400 kips, maximum strains of 0.18, 0.13 and 0.35 per cent were measured on the brackets of specimens 13A, 14A and 15A, respectively. When the load was increased to 600 kips, maximum axial strains of 0.53 and 0.38 per cent were measured on specimens 13A and 14A. At this load the gages on the highly stressed portion of 15A had been damaged. Extrapolation of the data taken at lower loads on specimen 15A indicated that strains exceeded one per cent at a load of 600 kips.

The strain distributions on the bottom plate under the freeing hole, section C-C, are shown in Figure 24 for specimens 13A, 14A and 15A. Strains in the mid-portion of the bottom plates, in line with the through-bracket plates, were appreciably higher than strains measured elsewhere in the bottom plates of the 13A design. The design of the freeing holes in the 15A specimen appeared to minimize the notch effect indicated in the 13A design. At 600 kips the strains under the freeing holes of the three 13A specimens (13A, 13AZ, and 14A ranged from 0.23 to 0.34 per cent and reached

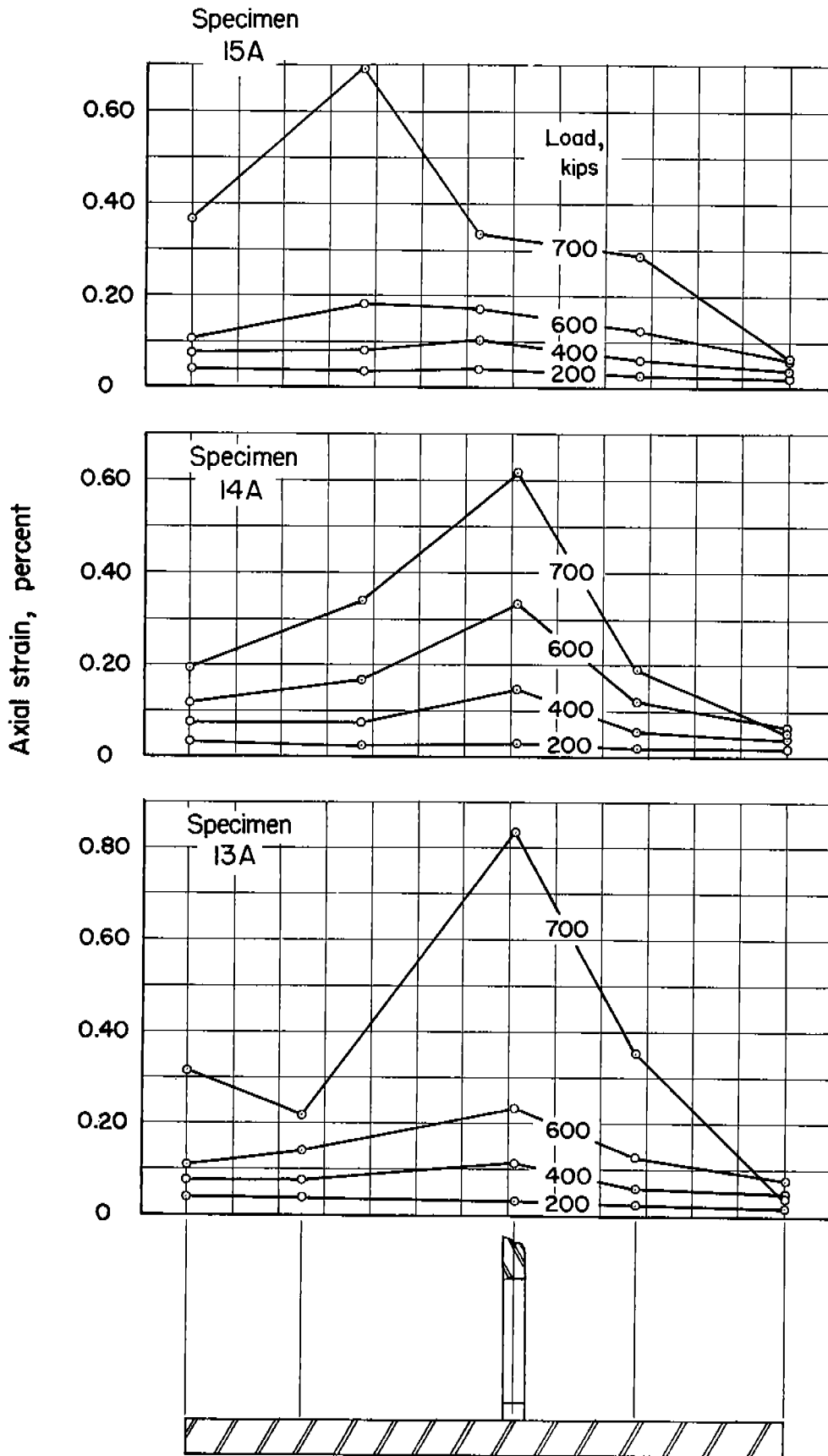


Fig. 24. Axial strain distributions on the bottom plate, section C-C, of specimens 13A, 14A and 15A.

0.17 per cent on specimen 15A. At these locations, strains on specimens 13A, 14A and 15A were 0.83, 0.62 and 0.33 per cent, respectively, at 700 kips. Edge strains in the center of the freeing holes, section C-C, reached 0.09 per cent for the 13A specimens and 0.74 per cent for specimen 15A at 600 kips. At 700 kips, these edge strains were 0.12 per cent for specimens 13A and 14A and 1.44 per cent for specimen 15A.

The distribution of the axial strains in the bottom plates and flanged longitudinals, section D-D, were determined for the through-bracket specimens and are shown in Figure 25 for specimens 13A, 14A and 15A. Strains across this section of the bottom plates did not vary greatly up to 700 kips. The maximum strains measured on bottom plate, section D-D, ranged from 0.12 to 0.21 per cent at 700 kips. Maximum strains in the flanged longitudinal were measured in the longitudinal webs 2 to 5 inches from the root of the formed flanges. Maximum strains in specimens 13A, 14A and 15A of 1.17, 0.75 and 0.19 per cent, respectively, were measured at 600 kips, and strains of 1.55, 1.14 and 0.36 per cent at 700 kips.

Axial strains were measured on the flat bar of specimen 15A approximately in line with the butt-weld joint. The strains at this section ranged from -0.09 to 0.62 per cent at 600 kips and from -0.25 to 1.33 per cent at 700 kips. The maximum values of strain were measured on the edge of the flat bar nearest the through-bracket.

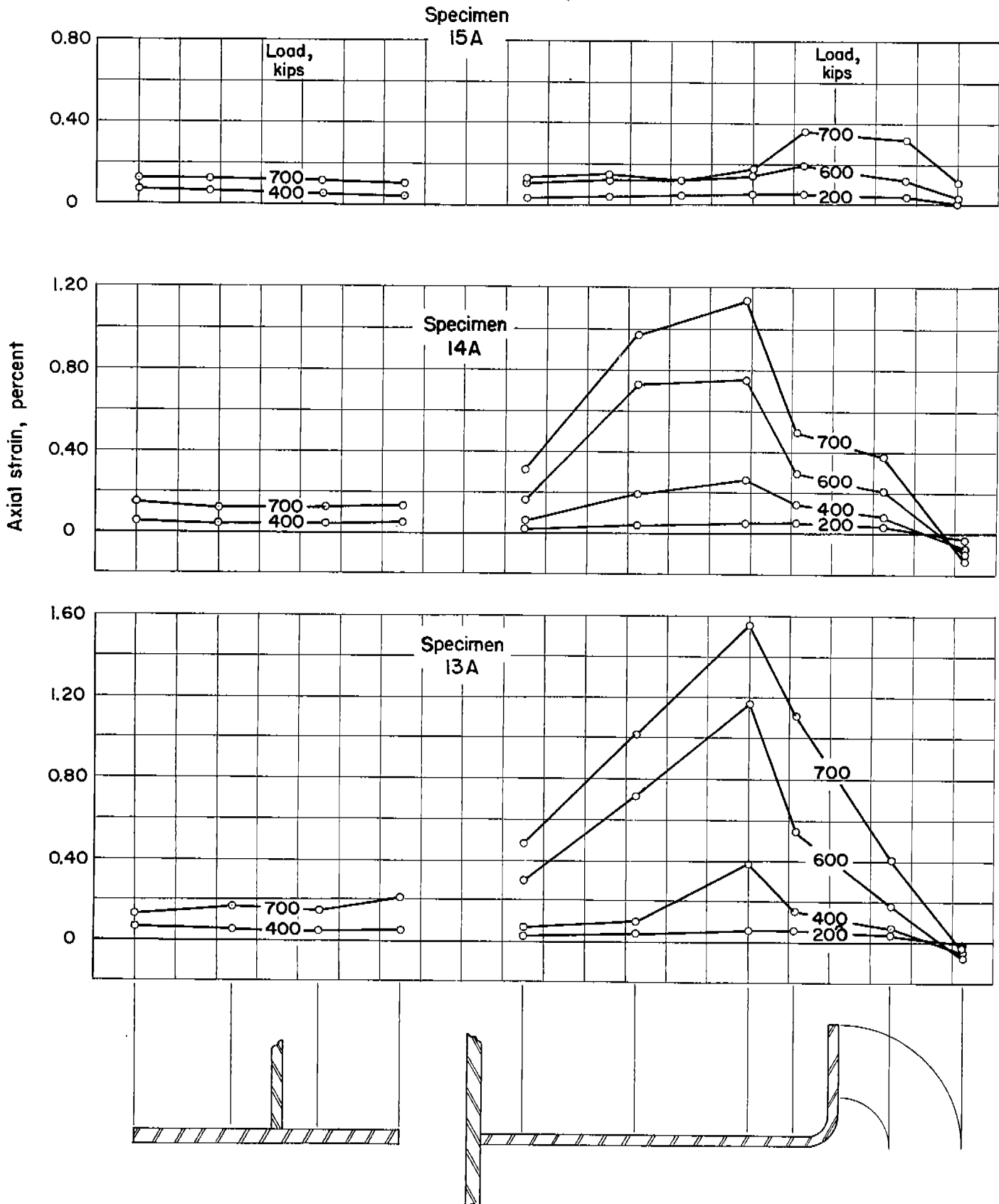


Fig. 25. Axial strain distributions on the bottom plate and longitudinal, section D-D, of specimens 13A, 14A and 15A.

The values of energy required to fracture the through-bracket longitudinal specimens were computed from the load versus axial extension relations. These values were adjusted proportionately to the ratio of the nominal cross-sectional area of the interrupted longitudinals outside the intersection to the comparable areas of the through-bracket specimens. The computed and adjusted values of energy are listed in Table 3. The adjusted energy to fracture values for specimens 13A, 14A and 15A were 107,200, 208,900 and 36,800 ft-lb, respectively. Specimens 14A and 15A fractured through the intersection, while on specimen 13A failure was at the connection to the pulling head. Determinations on specimen 13A2 were not comparable with other specimens for reasons previously discussed. The longitudinal design represented by specimens 13A and 14A appeared to be superior to the 15A design in ability to absorb the energy of deformation while sustaining tensile loads.

### 8. DISCUSSION OF RESULTS

The investigation of three discrete types of longitudinal connections at a transverse bulkhead was made to determine elastic stress distributions, strain distributions near failure, maximum load, and energy to fracture. The direction and magnitude of principal stresses, axial stress distributions and axial stress ratios were determined for one or more specimens of each design. Major principal stresses were larger in the region of and tended to converge on mechanical notches where

such notches were due to specimen geometry. The "hardspots" of stress were also evident in the axial distributions of the various specimens.

There was notable correlation of energy absorption to fracture with the maximum stress ratios found on section B-B adjacent to the transverse bulkhead. These stress ratios could be used to classify the specimen types using energy absorption as a measure of worth. That is, the stress ratios generally varied inversely with the energy absorption to fracture. At section B-B, a maximum stress ratio of 1.2 was measured on through longitudinal OA, maximum stress ratios ranging from 1.4 to 1.9 were measured on the through-bracket longitudinals (excluding 15A), and maximum stress ratios of from 2.1 to 2.8 were found for the interrupted longitudinals. A maximum stress ratio of 2.3 was measured on the bracket of specimen 15A. Comparisons of these values of stress ratio with corresponding values of energy to fracture, listed in Table 3, indicate that designs having the higher stress ratios on section B-B absorb less energy before fracture.

There was considerable scatter in results of the tests to failure. For any one design of longitudinal, this may be attributed to numerous factors, such as;

- (1) Variations in the mechanical properties of the material within plates and between plates from which specimens were fabricated.

- (2) Variations in chemical composition within and between plates.
- (3) Small dimensional differences between specimens of a given design.
- (4) Misalignment of component plates within the specimens and between the pulling heads and specimens.
- (5) Differences in the acuity of the notches, mechanical and metallurgical, due to the human element involved in making large weldments.

The maximum loads sustained by the different specimens ranged from 799 to 1,144 kips. Values of maximum load did not define the order of merit of the various specimen designs.

Plastic flow was measured on all specimens at loads substantially below the load corresponding to the proportional limit of a tensile bar of the same material and comparable cross section. At loads at which a tensile bar of cross section comparable with the appropriate specimen would have sustained 0.1 per cent strain, the average over-all strains were 0.13, 0.19 and 0.3 per cent for the through longitudinal, through-bracket longitudinals and interrupted longitudinals, respectively. Only those specimens tested to failure at temperatures near 0°F are compared. Except for specimens 12A and 15A, the change in average over-all strain due to increasing increments of load could be correlated with the maximum stress concentrations measured adjacent to the bulkhead. This indicates that the

localized plastic flow resulting from loads greater than 160 kips did not decrease the stress concentrations indicated by the elastic tests.

Openings in the longitudinal web at the bottom plate are necessary to provide drainage for the space between longitudinals. These openings unfortunately constitute a mechanical notch. At the higher loads, maximum strains in the bottom plates were measured in areas adjacent to these mechanical notches. Comparison of the maximum axial strains measured on the bottom plates of the through-bracket specimens with strains measured on the interrupted longitudinals shows that the acuity of the notches inherent in the interrupted design was diminished considerably by the through-bracket design. Maximum bottom plate strains of from 0.35 to 0.88 per cent at 700 kips were measured on the interrupted specimens, and strains of from 0.18 to 0.34 per cent were measured on bottom plates of the through-bracket specimens at 600 kips. The ratio of the cross-sectional areas of the interrupted longitudinals to the areas of the through-bracket longitudinals is nearly equal to the ratio of the loads 700 to 600 kips.

The large strains on the edges of the cutouts in the webs of interrupted longitudinal specimens of 2A design and on the edges of freeing holes in the through-bracket specimens probably are not significant criteria for selecting or rejecting a specific design. These regions of high strain

were relatively free from the constraints that existed at the sources of the brittle fractures in all specimens.

The tests to failure are thought to have been between the upper and lower transition temperatures for these structures as is indicated in Figure 21. The general trend for energy absorption to increase with temperature indicates that the energy absorption of a structure of given material is a function of its temperature over certain ranges. More extensive data and better control of the variables of material and workmanship are required to determine where and if upper and lower transition temperatures exist for this structure.

The load versus over-all extension curves for three accepted designs are compared with the load-extension curve of experimental design OA in Figure 26. The data represented by these curves were not adjusted to account for the differences in cross-sectional area of the specimens. On the basis of completed tests, these relationships represent the upper limit of load, extension and energy to fracture for interrupted longitudinal designs 1A and 2A and through-bracket design 13A when tested to failure near 0°F. The measured extensions of specimens 1A5, 2A, and 14A were 29, 38 and 50 per cent, respectively, of the extension measured for specimen OA. Comparisons of the adjusted energy to fracture values for these four specimens, Table 3, show that the energy to fracture for specimens 1A5, 2A and 14A was 20, 26 and 45 per cent, respectively, of the

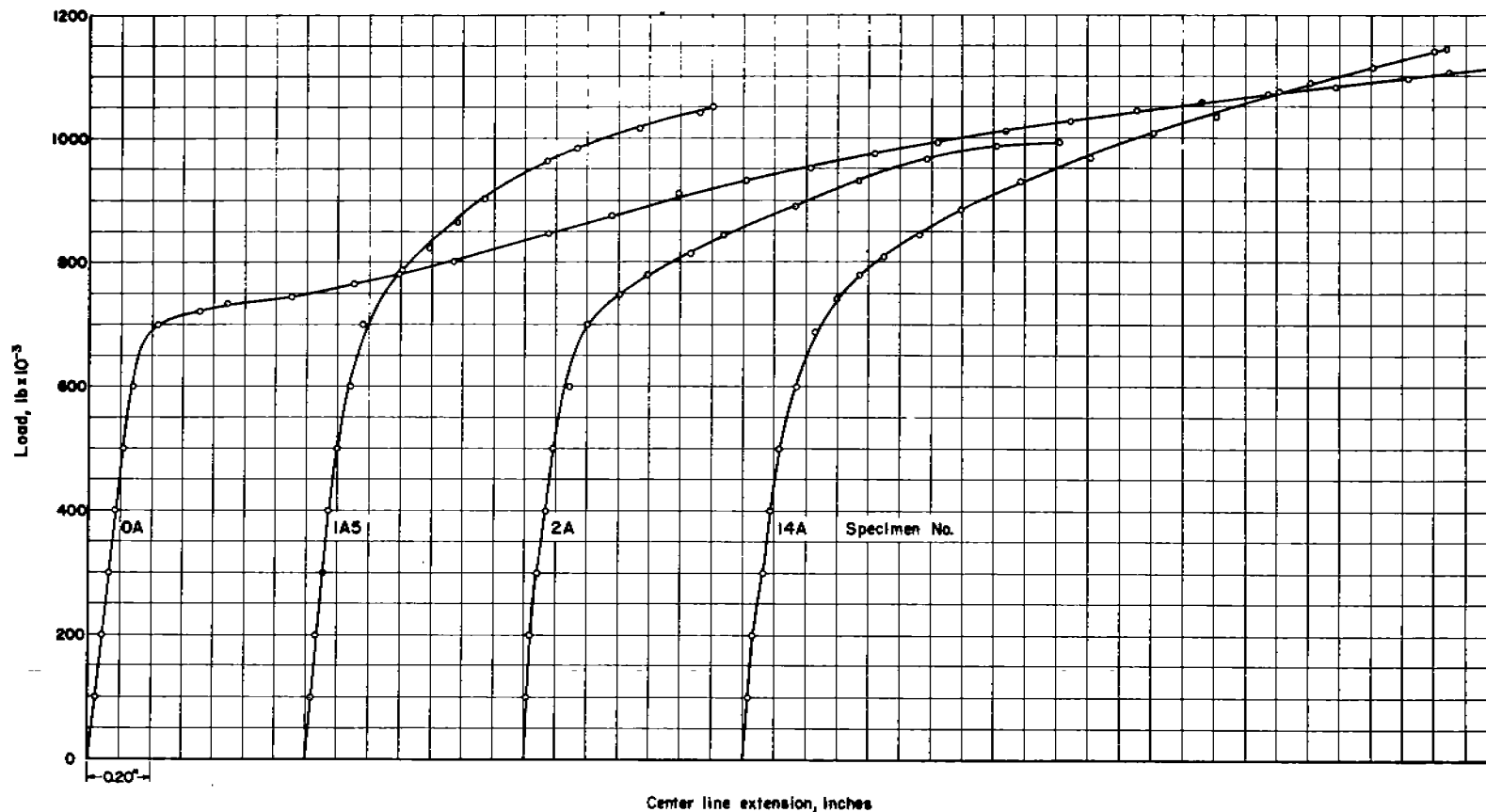


Fig. 26. Load versus over-all axial extension relations for specimens OA, 1A5, 2A and 14A. Data represented here were not adjusted for differences in cross-sectional area of specimens.

adjusted energy to fracture specimen OA. These comparisons of extension and energy to fracture point out the improvement of one through-bracket design over the interrupted designs and indicate the possibility of even better performance for this type structure.

As a measure of the over-all absorption of energy independent of specimen size, a method used by other investigators<sup>(7,8)</sup> may be employed to advantage. To make this comparison, the average energy absorption to rupture per cubic inch of material was computed for a number of specimens. The effective specimen length was taken as 100 inches, and the volume of material included only those components that sustained axial loads. These comparisons of energy absorption, using energy to fracture as the area under the load-extension curves in Figure 26, are listed below.

---

Specimen No.	OA	1A5	2A	14A
Energy Absorption, in.-lb per cu. in.	2180	390	500	870

---

The absence of stress raisers and freedom from some of the constraints inherent in the other designs are factors that contributed to the larger value of energy absorption determined for specimen OA.

## 9. SUMMARY

The nineteen specimens representing the intersection of a

flanged bottom longitudinal with a transverse bulkhead included one through longitudinal of experimental design, fourteen interrupted longitudinals comparable with T-2 tanker designs, and four through-bracket longitudinals, three of which were of one design of Navy oiler and one of a commercial tanker design.

The significant results of elastic tests of fourteen specimens at room temperature and tests to failure of nineteen specimens at low temperatures are summarized as follows:

- (1) The highest values of axial elongation, energy to fracture, and energy absorption per unit volume were associated with the experimental through longitudinal specimen 0A. Also, stresses and strains measured on this specimen at the section adjacent to the transverse bulkhead indicated the least notch effects or stress concentrations of the specimens investigated.
- (2) Modifications of the original 1A (T-2 tanker) design, which became the 2A design and the designs of specimens 3A and 12A, improved the performance of the structure as indicated by the values of maximum load, axial extension and energy to fracture.
- (3) The values of axial elongation, energy to fracture, and energy absorption per unit volume were generally higher for the Navy oiler design than for the T-2 tanker design. Also, the distribution of plastic

strains adjacent to the transverse bulkhead was more favorable in the oiler design.

- (4) The longitudinal representing a commercial tanker design compared unfavorably with the through-bracket design for Navy oilers and the better interrupted longitudinals, except that there was less notch effect on the bottom plate due to the details of the freeing holes. Results of tests of a single specimen, however, are not considered conclusive.
- (5) Maximum axial stress ratios (concentrations) measured adjacent to the transverse bulkhead in elastic tests can be correlated, qualitatively, with energy absorption capacity determined in tests to failure.
- (6) All specimens failed with cleavage fractures; thirteen specimens failed across the intersection being investigated and six specimens failed near the connection to the pulling heads.
- (7) Maximum loads sustained were not indicative of the order of merit for these structures.
- (8) Except for specimen OA, little or no change in plate thickness was measurable in the area of the fractures.
- (9) Energy to fracture versus temperature relations for eight 1A specimens point out the scatter of results in these tests and establish the general relationship

of higher values of energy to fracture with increased test temperature. Other specimens follow this same trend.

(10) The test temperatures were probably between the upper and lower transition temperatures for these structures.

(11) Large values of stress and strain measured on the edges of cutouts and freeing holes were not significant criteria for determining the ultimate worth of these designs.

#### 10. RECOMMENDATIONS FOR FUTURE WORK

The accepted designs of longitudinal intersections investigated in this laboratory did not utilize efficiently the maximum strength and ductility of the material from which they were fabricated. In cooperation with shipbuilders and operators, designers could make a coordinated attack on this problem and produce a small number of practical fundamental designs of this type of intersection. Prototypes of these designs could be evaluated under controlled conditions in order that designers can have a set of standard intersections of known advantages and limitations to serve as guides to solve particular problems.

It has come to the attention of the investigators that there is not now a means of analyzing the constraints to deformation inherent in built-up or compound structures. These constraints in the presence of stress concentrations appear to be

related to the initiation of brittle fractures in welded steel structures. Basic research that will yield quantitative results is needed. Connections in structures are neither 100 per cent constrained nor completely without constraint. Simplified models involving typical restraints could be evaluated experimentally and analytically. It appears that empirical and perhaps analytical methods and formulas could be developed from such an investigation that would permit designers to predict the operating characteristics of complex connections.

11. REFERENCES

1. Campbell, W. R. "Stress Studies of Welded Ship Structure Specimens", The Welding Journal, vol. 30, no. 2, Feb. 1951.
2. Campbell, W. R., Irwin, L. K., and Duncan, R. C. "Stress Studies of Bulkhead Intersections for Welded Tankers", The Welding Journal, vol. 31, no. 2, Feb. 1952.
3. "Considerations of Welded Hatch Corner Design", Ship Structure Committee Report Serial no. SSC-37, Oct. 1, 1952.
4. Baumberger, R., and Hines, F. "Practical Reduction Formulas for use on Bonded Wire Strain Gages in Two-Dimensional Stress Fields", Proc. Soc. Exp. Stress Anal., vol II, no. 1 (1944).
5. Timoshenko, S. "Strength of Materials", Part I, D. Van Nostrand Co.: New York, (June, 1940). Pp. 44--52.
6. Brock, J. S., and Eder, J. P. "Stresses in a Photoelastic Model of a Bottom Longitudinal Connection at a Bulkhead in Navy Oilers", Department of the Navy, David Taylor Model Basin Report 851, Feb. 1953.
7. Roop, W. P. Discussion of ref. 2, The Welding Journal, vol. 31, no. 2, pp. 75s--76s, Feb. 1952.
8. Carpenter, S. T., and Roop, W. P. "Final Report on the Strength, Energy Absorption and Transition Temperature of Internally Notched Flat Steel Plates"; Ship Structure Committee Report Serial no. SSC-47, Jan. 19, 1953.

## 12. APPENDIX

Carbon steel plates rolled from one heat were acquired at the beginning of the investigation of bulkhead inter-sections. Most of this supply of material was exhausted during fabrication of the eight specimens for the preliminary tests, results of which were published earlier. The 30.6# bottom plate material for the nineteen specimens considered in this report and the 40.8# bracket material for specimen 1A were from this original stock of material. Silicon killed steel from 40.8# plate was used for the brackets of the other interrupted longitudinals. All 20.4# material used in these nineteen specimens was from yard stock ship plate. It is thought that the 40.8# flat bar material in specimen 15A was also yard stock.

The chemical compositions of samples taken from various plates are given in Table 4. These plates appear to have been rolled from semi-killed ingots with carbon and manganese as the alloying elements except for the 30.6# bottom plate in specimen 2A2 and the 40.8# bracket material for the interrupted specimens. Test results of specimen 2A2 indicated that the material used in its fabrication had properties different from those of previous specimens. A subsequent chemical analysis, Table 4, indicated that the bottom plate was nearly pure iron with manganese the only important alloying element detected. The compositions of the 20.4# plates for specimens 2A2 and

Table 4. Chemical Composition of Plates in Nineteen Longitudinal Specimens

Component	Specimen	C	Mn*	P	S	Si*	Ni*	Cr**	Mo**	V*	Cu**	Ti*	Al*	N	Lab.
Percent															
20.4# Long'l	15A	.23	.52	.005	.034	.057	.040	.019	.021	Tr	.036	Tr	.01	.004	NBS
20.4# Long'l	2A2	.13	.41	.004	.029	.022	.15	.03	.012	Tr	.32	Tr	Tr	----	NBS
30.6# Bott. Pl.	All spec. except 2A2	.25	.42	.009	.025	.08	.07	.09	.05	.007	.02	.004	.003	.004	NYNSY
30.6# Bott. Pl.	2A2	.04	.36	.004	.009	Tr	.07	.02	.005	Tr	.05	Tr	Tr	----	NBS
40.8# Bracket	1A	.24	.42	.009	.025	.08	.07	.09	.05	.007	.02	.004	.003	.004	NYNSY
40.8# Bracket	Interrupted specimens except 1A	.21	.68	.016	.022	.22	.05	.02	.02	.005	.11	.004	.003	.005	NYNSY
40.8# Flat Bar	15A	.24	.44	.007	.037	.080	.047	.082	.003	.Tr	.036	Tr	.01	.003	NBS

\*Spectrochemical analysis.

15A are thought to be representative of the other 20.4# plates used in this investigation.

The mechanical properties of some of the plates used in these specimens are listed in Table 5. These plates had the characteristic properties of carbon-manganese ship plate except the 30.6# bottom plate of specimen 2A2. The values of yield strength and reduction of area determined for this plate were influenced by the test to failure of specimen 2A2.

The tensile strength of this plate, 47,900 lb. per. sq. in., indicated that the material in this specimen had less strength than normal ship plate.

Table 5. Mechanical Properties of Steel Plates in Nineteen Longitudinal Specimens

Component	Specimen	Yield Point	Tensile Strength	Elong. in 2 in.	Elong. in 8 in.	Reduction in Area	Young's Modulus	Trans. Temp.*	Lab.
		lb/in <sup>2</sup>	lb/in <sup>2</sup>	percent	percent	percent	lb/in <sup>2</sup>	°F	
20.4# Long'l	15A	38,800	63,000	----	30.4	55.0	30,100,000	----	NBS
30.6# Bott. Pl.	All spec. except 2A2	-- ---	-- ---	----	----	----	-- --- ---	100	NYNSY
30.6# Bott. Pl.	2A2	35,900+	47,900	29.5+	----	----	-- --- ---	----	NBS
30.6# Bott. Pl.	15A	32,200	64,000	----	25.4	50.2	30,200,000	----	NBS
40.8# Bracket	1A	-- ---	-- ---	----	----	----	-- --- ---	120	NYNSY
40.8# Bracket	Interrupted specimens except 1A	42,000	64,400	37.5	----	65.7	-- --- ---	110	NYNSY
40.8# Flat Bar	15A	30,100	60,700	----	32.4	52.4	29,400,000	----	NBS

\* Transition temperature as determined by the Navy Tear Test

+ Values affected by preload of 918 kips required to fracture specimen 2A2